
Deep learning for cardiac image segmentation: A review

Chen Chen^{1,*}, Chen Qin^{1,*}, Huaqi Qiu^{1,*}, Giacomo Tarroni^{1,2}, Jinming Duan³, Wenjia Bai^{4,5}, and Daniel Rueckert¹

¹ *Biomedical Image Analysis Group, Department of Computing, Imperial College London, London, UK;*

² *Department of Computer Science, City, University of London, London, UK;*

³ *School of Computer Science, University of Birmingham, Birmingham, UK;*

⁴ *Data Science Institute, Imperial College London, London, UK;*

⁵ *Division of Brain Sciences, Department of Medicine, Imperial College London, London, UK*

Correspondence*:

Chen Chen

chen.chen15@imperial.ac.uk

ABSTRACT

Deep learning has become the most widely used approach for cardiac image segmentation in recent years. In this paper, we provide a review of over 100 cardiac image segmentation papers using deep learning, which covers common imaging modalities including magnetic resonance imaging (MRI), computed tomography (CT), and ultrasound (US) and major anatomical structures of interest (ventricles, atria and vessels). In addition, a summary of publicly available cardiac image datasets and code repositories are included to provide a base for encouraging reproducible research. Finally, we discuss the challenges and limitations with current deep learning-based approaches (scarcity of labels, model generalizability across different domains, interpretability) and suggest potential directions for future research.

Keywords: Artificial intelligence, deep learning, neural networks, cardiac image segmentation, cardiac image analysis, MRI, CT, US

ARTICLE TYPES

Review

1 INTRODUCTION

Cardiovascular diseases (CVDs) are the leading cause of death globally according to World Health Organization (WHO). About 17.9 million people died from CVDs in 2016, from CVD, mainly from heart disease and stroke¹. The number is still increasing annually. In recent decades, major advances have been made in cardiovascular research and practice aiming to improve diagnosis and treatment of cardiac diseases as well as reducing the mortality of CVD. Modern medical imaging techniques such as magnetic resonance imaging (MRI), computed tomography (CT) and ultrasound (US) are now widely used, which enable non-invasive qualitative and quantitative assessment of cardiac anatomical structures and functions and provide support for diagnosis, disease monitoring, treatment planning and prognosis.

Of particular interest, cardiac image segmentation is an important first step in numerous applications. It partitions the image into a number of semantically (i.e. anatomically) meaningful regions, based on which quantitative measures can be extracted, such as the myocardial mass, wall thickness, left

¹ https://www.who.int/cardiovascular_diseases/about_cvd/en/

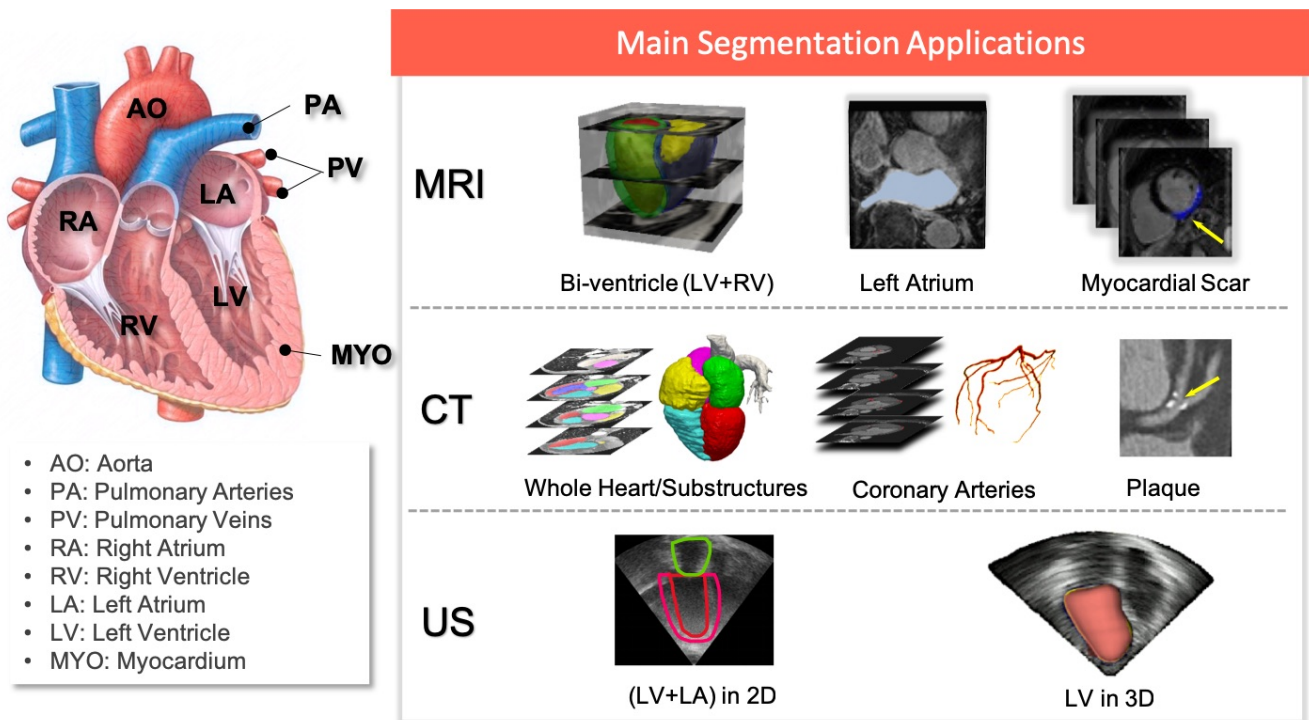


Figure 1. Overview of cardiac image segmentation tasks for different imaging modalities. For better understanding, we provide the anatomy of the heart on the left (image source: clipart-library.com). Of note, for simplicity, we list the tasks for which deep learning techniques have been applied, which will be discussed in Section 3.

ventricle (LV) and right ventricle (RV) volume as well as ejection fraction (EF) etc. Typically, the anatomical structures of interest for cardiac image segmentation include the LV, RV, left atrium (LA), right atrium (RA), and coronary arteries. An overview of typical tasks related to cardiac image segmentation is presented in Fig. 1, where applications for the three most commonly used modalities, i.e., MRI, CT and US, are shown.

Before the rise of deep learning, traditional machine learning techniques such as model-based methods (e.g. active shape and appearance models) and atlas-based methods had been shown to achieve good performance in cardiac image segmentation (Petitjean et al., 2015; Peng et al., 2016; Tavakoli and Amini, 2013; Lesage et al., 2009). However, they often require significant feature engineering or prior knowledge to achieve satisfactory accuracy. In contrast, deep learning (DL)-based algorithms are good at *automatically* discovering intricate features from data for object detection and segmentation. These features are directly learned from data using

a general-purpose learning procedure and in end-to-end fashion. This makes DL-based algorithms easy to apply to other image analysis applications. Benefiting from advanced computer hardware (e.g. graphical processing units (GPUs) and tensor processing units (TPUs)) as well as increased available data for training, DL-based segmentation algorithms have gradually outperformed previous state-of-the-art traditional methods, gaining more popularity in research. This trend can be observed in Fig. 2A, which shows how the number of DL-based papers for cardiac image segmentation has increased strongly in the last years. In particular, the number of the publications for MR image segmentation is significantly higher than the numbers of the other two domains, especially in 2017. One reason, which can be observed in Fig. 2B, is that the publicly available data for MR segmentation has increased remarkably since 2016.

In this paper, we provide an overview of state-of-the-art deep learning techniques for cardiac image segmentation in the three most

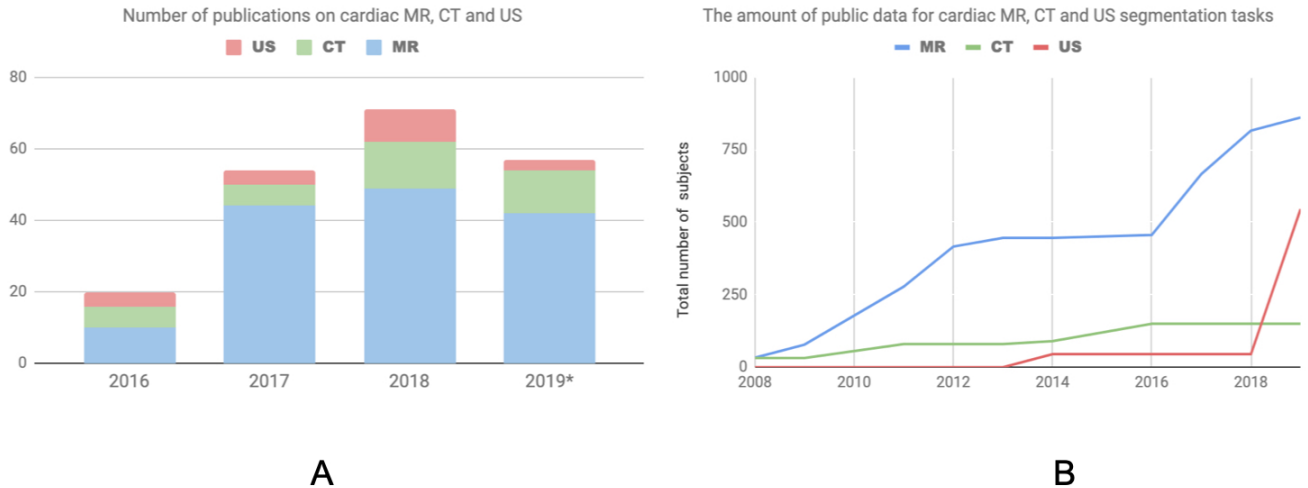


Figure 2. (A) Overview of numbers of papers published from 1st January 2016 to 1st August 2019 regarding deep learning-based methods for cardiac image segmentation reviewed in this work. (B) The increase of public data for cardiac image segmentation in the past ten years. CT: computed tomography, MR: magnetic resonance, US: ultrasound.

commonly used modalities (i.e. MRI, CT, US) in clinical practice and discuss the advantages and remaining limitations of current deep learning-based segmentation methods that hinder widespread clinical deployment. To our knowledge, there have been several review papers that presented overviews about applications of DL-based methods for general medical image analysis (Greenspan et al., 2016; Shen et al., 2017; Litjens et al., 2017), as well as some surveys dedicated to applications designed for cardiovascular image analysis (Gandhi et al., 2018; Mazurowski et al., 2019). However, none of them has provided a systematic overview focused on *cardiac segmentation applications*. This review paper aims at providing a comprehensive overview from the debut to the state-of-the-art of deep learning algorithms, focusing on a variety of cardiac image segmentation tasks (e.g. the LV, RV, and vessel segmentation) (Sec. 3). Particularly, we aim to cover most influential DL-related works in this field published until 1st August 2019 and categorized these publications in terms of specific methodology. Besides, in addition to the basics of deep learning introduced in Sec.2, we also provide a summary of public datasets (see Table 6) as well as public code (see Table 7), aiming to present a good reading basis for newcomers to the topic and

encourage future contributions. More importantly, we provide insightful discussions about the current research situations (Sec.3.4) as well as challenges and potential directions for future work (Sec. 4).

Search criterion To identify related contributions, search engines like Scopus and PubMed were queried for papers containing (“convolutional” OR “deep learning”) and (“cardiac”) and (“image segmentation”) in title or abstract. Additionally, conference proceedings for MICCAI, ISBI and EMBC were searched based on the titles of papers. Papers which do not primarily focus on segmentation problems were excluded. The last update to the included papers was on Aug 1, 2019.

2 FUNDAMENTALS OF DEEP LEARNING

Deep learning models are deep artificial neural networks. Each neural network consists of an input layer, an output layer, and multiple hidden layers. In the following section, we will review several deep learning networks and key techniques that have been commonly used in state-of-the-art segmentation algorithms. For a more detailed and thorough illustration of the mathematical

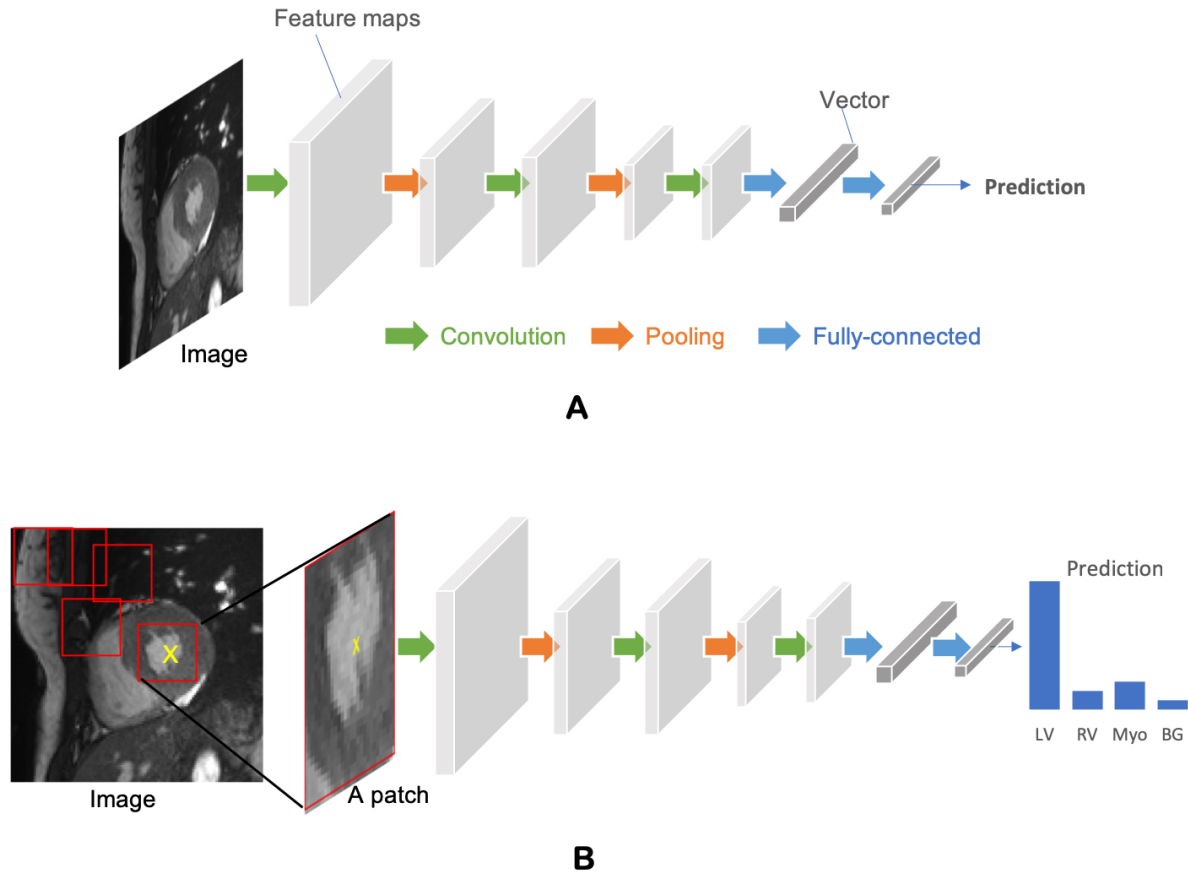


Figure 3. (A) Generic architecture of convolutional neural networks (CNN). A CNN takes a cardiac MR image as input, learning hierarchical features through a stack of convolutions and pooling operations. These spatial feature maps are then flattened and reduced into a vector through fully connected layers. This vector can be in many forms, depending on the specific task. It can be probabilities for a set of classes (image classification) or coordinates of a bounding box (object localization) or a predicted label for the center pixel of the input (patch-based segmentation) or a real value for regression tasks (e.g. left ventricular volume estimation). **(B) Patch-based segmentation method based on a CNN classifier.** The CNN takes a patch as input and outputs the probabilities for four classes where the class with the highest score is the prediction for the center pixel (see the yellow cross) in this patch. By repeatedly forwarding patches located at different locations into the CNN for classification, one can finally get a pixel-wise segmentation map for the whole image. LV:left ventricle; RV: right ventricle; BG: Background; Myo: left ventricular myocardium.

background and fundamentals of deep learning we refer the interested reader to Goodfellow (2016).

2.1 Neural Networks

In this section, we first introduce basic neural network architectures and then briefly introduce building blocks which are commonly used to boost the ability of the networks to learn features that are useful for image segmentation.

2.1.1 Convolutional Neural Networks (CNNs)

In this part, we will introduce convolutional neural network (CNN), which is the most common type of deep neural networks for image analysis. CNN have been successfully applied to advance the state-of-the-art on many image classification, object detection and segmentation tasks.

As shown in Fig. 3A, a standard CNN consists of an input layer, an output layer and a stack of functional layers in between that transform an input

into an output in a specific form (e.g. vectors). These functional layers often contains convolutional layers, pooling layers and/or fully-connected layers. In general, each convolution uses a $n \times n$ kernel (for 2D input) or $n \times n \times n$ kernel (for 3D input) followed by batch normalization (Ioffe and Szegedy, 2015) after which the output is passed through a nonlinear activation function (e.g. rectified linear unit (ReLU)), which is used to extract feature maps from an image. These feature maps are then downsampled by pooling layers, typically by a factor of 2, which removes redundant features to improve the statistical efficiency and model generalization. After that, fully connected layers are applied to reduce the dimension of features and find the most task-relevant features for inference. The output of the network is a fix-sized vector where each element can be a probabilistic score for each category (for image classification), a real value for a regression task (e.g. the left ventricular volume estimation) or a set of values (e.g. the coordinates of a bounding box for object detection and localization).

In general, the size of convolution kernel n is chosen to be small in general, e.g. $n = 3$, in order to reduce computational costs. While the kernels are small, one can increase the receptive field (the area of the input image that potentially impacts the activation of a particular convolutional kernel/neuron) by increasing the number of convolutional layers. For example, a convolutional layer with large 7×7 kernels can be replaced by three layers with small 3×3 kernels. The number of parameters is reduced by a factor of $7^2 / (3 \times (3^2)) \approx 2$ while the receptive field remains the same (7×7). An online resource² is referred here, which illustrates and visualizes the change of receptive field by varying the number of hidden layers and the size of kernels. In general, increasing the depth of convolution neural networks (the number of hidden layers) to enlarge the receptive field can lead to improved model performance, e.g.

classification accuracy (Simonyan and Zisserman, 2015).

CNNs for image classification can also be employed for image segmentation applications without major adaptations to the network architecture (Ciresan and Giusti, 2012), as shown in Fig. 3B. However, this requires to divide each image into patches and then train a CNN to predict the class label of the center pixel for every patch. One major disadvantage of this patch-based approach is that, at inference time, the network has to be deployed for every patch individually despite the fact that there is a lot of redundancy due to multiple overlapping patches in the image. As a result of this inefficiency, the main application of CNNs with fully connected layers is object localization, which aims to estimate the bounding box of the object of interest in an image. This bounding box is then used to crop the image, forming an image pre-processing step to reduce the computational cost for segmentation (Avendi et al., 2016). For efficient, end-to-end pixel-wise segmentation, a variant of CNNs called fully convolutional neural network (FCN) is more commonly used, which will be discussed in the next section.

2.1.2 Fully Convolutional Neural Networks (FCNs)

The idea of FCN was first introduced by Long et al. (2015) for image segmentation. FCNs are a special type of CNNs that do not have any fully connected layers. In general, as shown in Fig. 4A, FCNs are designed to have an encoder-decoder structure such that they can take input of arbitrary size and produce the output with the same size. Given an input image, the encoder first transforms the input into high-level feature representation whereas the decoder interprets the feature maps and recovers spatial details back to the image space for pixel-wise prediction through a series of transposed convolution and convolution operations. Here, transposed convolutions are used for up-scaling the feature maps, typically by a factor of 2. These transposed convolutions can also be replaced by unpooling layers and upsampling layers.

² <https://fomoro.com/research/article/receptive-field-calculator>

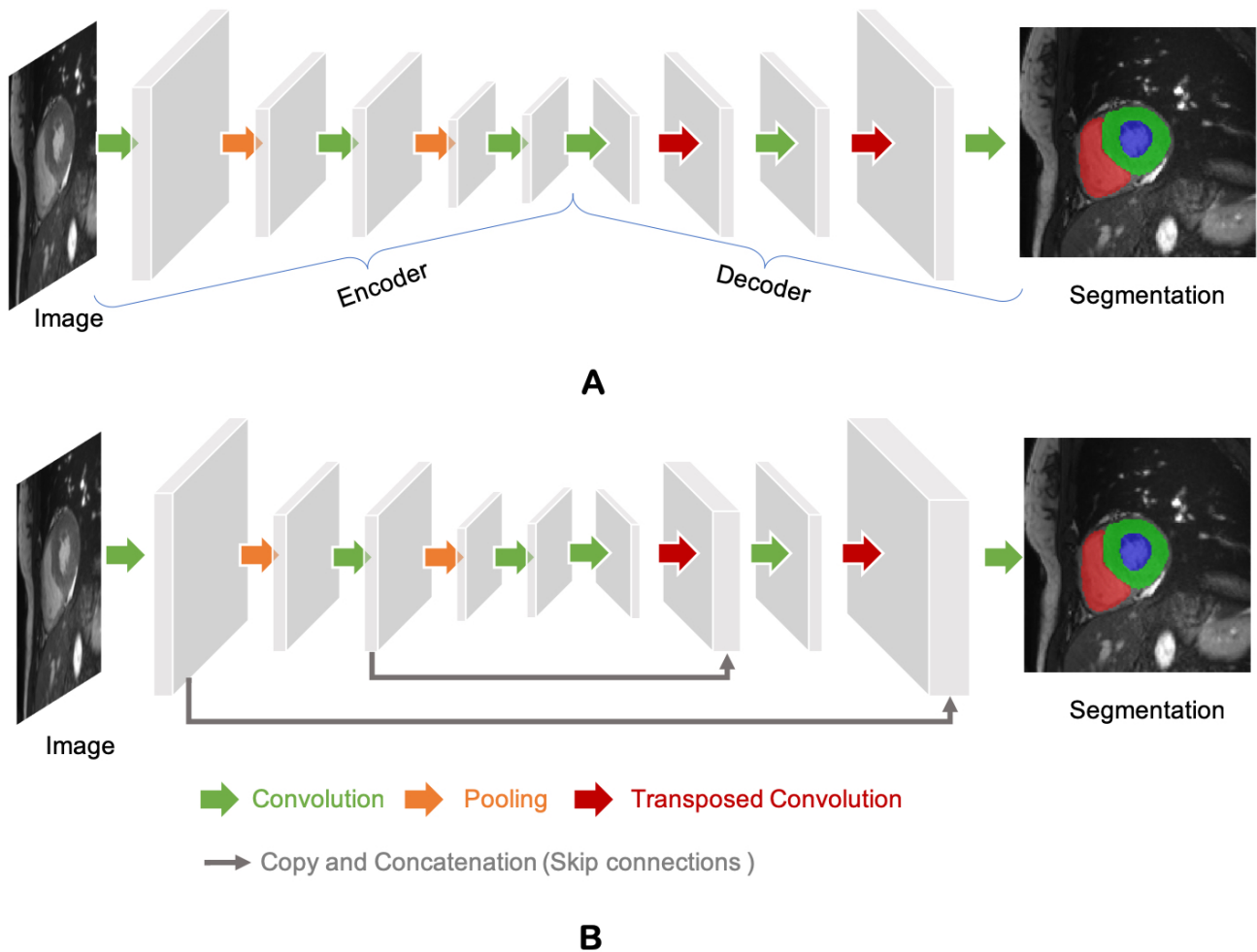


Figure 4. (A) Generic architecture of fully convolutional neural networks (FCN) for segmentation. The FCN first takes the whole image as input, learns deep image features through the encoder, gradually recovers the spatial dimension by a series of transposed convolution layers in the decoder and finally predicts a pixel-wise image segmentation for the left ventricle cavity (the blue region), the left ventricular myocardium (the green region) and the right ventricle (the red region). One use case of this FCN-based cardiac segmentation can be found in Tran (2016). **(B) A schematic drawing of U-net.** On the basis of the basic structure of FCN, U-net employs ‘skip connections’ (the gray arrows) to aggregate feature maps from coarse to fine. Of note, for simplicity, we reduce the number of downsampling and upsampling blocks. For detailed information, we recommend readers to the original paper (Ronneberger and Brox, 2015).

Compared to a patch-based CNN for segmentation, FCN is trained and applied to the entire images, removing the need for patch selection (Shelhamer et al., 2017).

FCN with the simple encoder-decoder structure in Fig. 4A may be limited to capture detailed context information in an image for precise segmentation as some features may be eliminated by the pooling layers in the encoder. Several variants of FCNs have been proposed to propagate features from

the encoder to the decoder, in order to boost the segmentation accuracy. The most well-known and most popular variant of FCNs for biomedical image segmentation is the U-net (Ronneberger and Brox, 2015). On the basis of the vanilla FCN (Long et al., 2015), the U-net employs skip connections between the encoder and decoder to recover spatial context loss in the down-sampling path, yielding more precise segmentation (see Fig. 4B). Several state-of-the-art cardiac image segmentation methods have

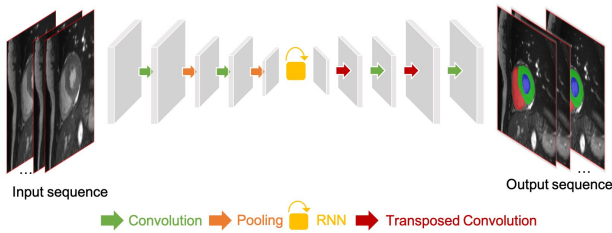


Figure 5. An example of RNN for cardiac image segmentation. The yellow block with a curved arrow represents a RNN module, which can memorize the past and use the knowledge learned from the past to make its present decision. This type of network is ideal for sequential data such as cine MR images and ultrasound movies, as well as volumetric data. In this example, the network is used to segment cardiac ventricles from a stack of 2D cardiac MR slice, which allows to propagate contextual information from adjacent slices in the z-direction for better inter-slice coherence (Poudel et al., 2016).

adopted the U-net or its 3D variants, the 3D U-net (Çiçek et al., 2016) and the 3D V-net (Milletari et al., 2016), as their backbone networks, achieving promising segmentation accuracy for a number of cardiac segmentation tasks (Tao et al., 2019; Isensee et al., 2017; Xia et al., 2018).

2.1.3 Recurrent Neural Networks (RNNs)

Recurrent neural networks (RNNs) are another type of artificial neural networks which are used for sequential data, such as cine MRI and ultrasound image sequences. An RNN can ‘remember’ the past and use the knowledge learned from the past to make its present decision, see Fig 5. For example, given a sequence of images, an RNN takes the first image as input, captures the information to make a prediction and then memorize this information which is then utilized to make a prediction for the next image. The two most widely used architectures in the family of RNNs are LSTM (Hochreiter and Schmidhuber, 1997) and gated recurrent unit (GRU) (Cho et al., 2014), which are capable of modeling long-term memory. A use case for cardiac segmentation is to combine an RNN with a 2D FCN so that the combined network is capable of capturing information from adjacent slices to

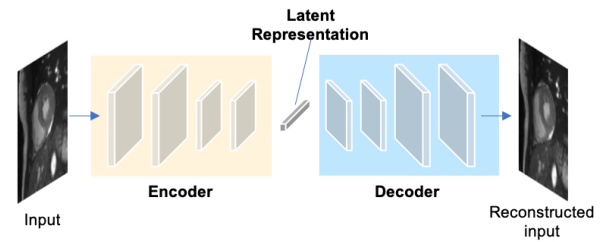


Figure 6. A generic architecture of an autoencoder. An autoencoder employs an encoder-decoder structure, where the encoder maps the input data to a low-dimensional latent representation and the decoder interprets the code and reconstructs the input.

improve the inter-slice coherence of segmentation results (Poudel et al., 2016).

2.1.4 Autoencoders (AE)

Autoencoders (AEs) are a type of neural networks that are designed to learn compact latent representations from data without supervision. A typical architecture of an autoencoder consists of two networks: an encoder network and a decoder network for the reconstruction of the input, see Fig. 6. Since the learned representations contain generally useful information in the original data, many researchers have employed autoencoders to extract general semantic features or shape information from input images or labels and then use those features to guide the cardiac image segmentation (Oktay et al., 2016; Schlemper et al., 2018; Yue et al., 2019).

2.1.5 Generative Adversarial Networks (GAN)

The concept of Generative adversarial network (GAN) was proposed by Goodfellow et al. (2014) for image synthesis from noise. GANs are a type of generative models that learn to model the data distribution of real data and thus are able to create new image examples. As shown in Fig. 7A, a GAN consists of two networks: a generator network and a discriminator network. During training, the two networks are trained to compete against each other: the generator produces fake images aimed at fooling the discriminator, whereas the discriminator tries to

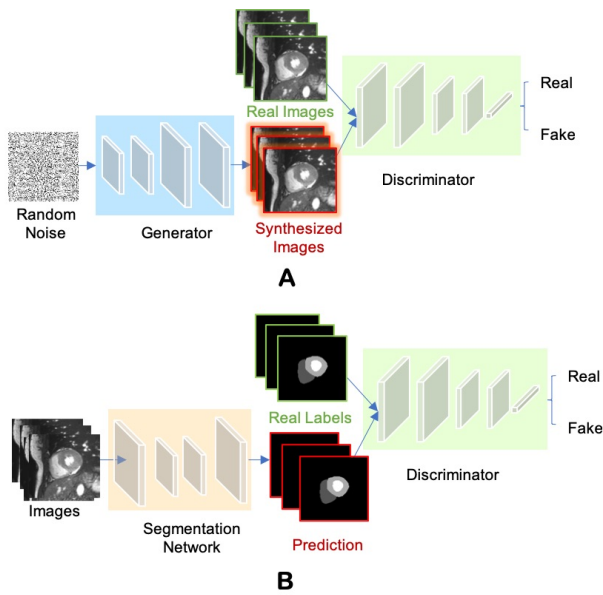


Figure 7. (A) Overview of GAN for image synthesis; (B) Overview of adversarial training for image segmentation.

identify real images from fake ones. This type of training is referred to as ‘adversarial training’, since the two models are both set to win the competition. This training scheme can also be used for training a segmentation network. As shown in Fig. 7B, the generator is replaced by a segmentation network and the discriminator is required to distinguish the generated segmentation maps from the ground truth ones (the target segmentation maps). In this way, the segmentation network is encouraged to produce more anatomically plausible segmentation maps (Luc et al., 2016; Savioli et al., 2018).

2.1.6 Advanced building blocks for improved segmentation

Medical image segmentation, as an important step for quantitative analysis and clinical research, requires a pixel-wise accuracy. Over the past years, many researchers have developed advanced building blocks to learn robust, representative features for precise segmentation. These techniques have been widely applied to state-of-the-art neural networks (e.g. U-net) to improve cardiac image segmentation performance. Therefore, we identified several important techniques reported in the literature to this end and present them with corresponding

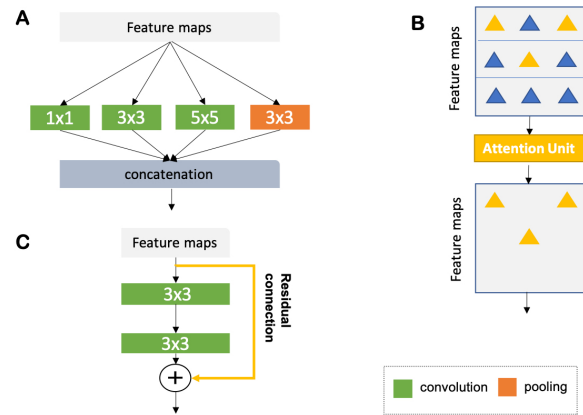


Figure 8. (A) Naive version of the inception module (Szegedy et al., 2015). In this module, convolutional kernels with varying sizes are applied to the same input for multi-scale feature fusion. (B) Schematic diagram of the attention module (Vaswani et al., 2017; Oktay et al., 2018b). The attention module teaches the network to pay attention to important features (e.g. features relevant to anatomy) and ignore redundant features. (C) Schematic diagram of a residual unit (He et al., 2016). The yellow arrow represents a residual connection which is applied to reusing the features from the previous layer. The numbers in the green and orange blocks denote the sizes of corresponding convolutional or pooling kernels. Here, for simplicity, all diagrams have been reproduced based on the illustration in the original papers.

references for further reading. These techniques are:

- Advanced convolutional modules for multi-scale feature aggregation in the hidden layers:
 - Inception modules (Szegedy et al., 2015), see Fig. 8A;
 - Dilated convolutional kernels (Yu and Koltun, 2016);
 - Deep supervision (Lee et al., 2015);
 - Atrous spatial pyramid pooling (Chen et al., 2017);
- Adaptive convolutional kernels designed to pay attention to important features:
 - Attention units (Vaswani et al., 2017), see Fig. 8B;

- Squeeze-and-excitation blocks (Hu et al., 2018);
3. Interlayer connections designed to reuse features from previous layers:
- Residual connections (He et al., 2016), see Fig. 8C;
 - Dense connections (Huang et al., 2017).

2.2 Training Neural Networks

Before being able to perform inference, neural networks must be trained. This training process requires a dataset that contains paired images and labels $\{\mathbf{x}, \mathbf{y}\}$ for training and testing, an optimizer (e.g. stochastic gradient descent, Adam) and a loss function to update the model parameters. This function accounts for the error of the network prediction in each iteration during training, providing signals for the optimizer to update the network parameters through backpropagation. The goal of training is to find proper values of the network parameters to minimize the loss function.

2.2.1 Common Loss Functions

For regression tasks (e.g. heart localization, calcium scoring, landmark detection, image reconstruction), the simplest loss function is the mean squared error (MSE):

$$\mathcal{L}_{\text{MSE}} = \frac{1}{n} \sum_{i=1}^n (\mathbf{y}_i - \hat{\mathbf{y}}_i)^2, \quad (1)$$

where \mathbf{y}_i is the vector of target values and $\hat{\mathbf{y}}_i$ is the vector of the predicted values; n is the number of data samples.

Cross-entropy is the most common loss for both image classification and segmentation tasks. In particular, the cross-entropy loss for segmentation summarizes the pixel-wise probability errors between the predicted probabilistic output \mathbf{p} and its corresponding target segmentation map \mathbf{y} for each class c :

$$\mathcal{L}_{\text{CE}} = -\frac{1}{n} \sum_{i=1}^n \sum_{c=1}^C \mathbf{y}_i^c \log(\mathbf{p}_i^c), \quad (2)$$

where C is the number of all classes. Another loss function which is specifically designed for object segmentation is called soft-Dice loss function (Milletari et al., 2016), which penalizes the mismatch between a predicted segmentation map and its target map at pixel-level:

$$\mathcal{L}_{\text{Dice}} = 1 - \frac{2 \sum_{i=1}^n \sum_{c=1}^C \mathbf{y}_i^c \mathbf{p}_i^c}{\sum_{i=1}^n \sum_{c=1}^C (\mathbf{y}_i^c + \mathbf{p}_i^c)}. \quad (3)$$

In addition, there are several variants of the cross-entropy or soft-Dice loss such as the weighted cross-entropy loss (Jang et al., 2017; Baumgartner et al., 2017) and weighted soft-Dice loss (Yang et al., 2017c; Khened et al., 2019) that are used to address potential class imbalance problem in medical image segmentation tasks where the loss term is weighted to account for rare classes or small objects.

2.2.2 Reduce over-fitting

The biggest challenge of training deep networks for medical image analysis is over-fitting, due to the fact that there is often a limited number of training images in comparison with the number of learnable parameters in a deep network. A number of techniques have been developed to alleviate this problem. Some of the techniques are the following ones:

- Weight initialization (He et al., 2015) and weight regularization (i.e. L1/L2 regularization)
- Dropout (Srivastava et al., 2014)
- Ensemble learning (Kamnitsas et al., 2017a)
- Data augmentation by artificially generating training samples via affine transformations
- Transfer learning with a model pre-trained on existing large datasets.

2.3 Evaluation Metrics

To quantitatively evaluate the performance of automated segmentation algorithms, three types of metrics are commonly used: a) volume-based metrics (e.g. Dice metric, Jaccard similarity index); b) surface distance-based metrics (e.g. mean

contour distance, Hausdorff distance); c) clinical performance metrics (e.g. ventricular volume and mass). For a detailed illustration of common used clinical indices in cardiac image analysis, we recommend the review paper by Peng et al. (2016). In our paper, we mainly report the accuracy of methods in terms of the Dice metric for ease of comparison. The Dice score measures the ratio of overlap between two results (e.g. automatic segmentation vs manual segmentation), ranging from 0 (mismatch) to 1 (perfect match).

3 DEEP LEARNING FOR CARDIAC IMAGE SEGMENTATION

In this section, we provide a summary of deep learning-based applications for the three main imaging modalities: MRI, CT, and US regarding specific applications for targeted structures. In general, these deep learning-based methods provide an efficient and effective way to segmenting particular organs or tissues (e.g. the LV, coronary vessels, scars) in different modalities, facilitating follow-up quantitative analysis of cardiovascular structure and function. Among these works, a large portion of these methods are designed for ventricle segmentation, especially in MR and US domains. The objective of ventricle segmentation is to delineate the endocardium and epicardium of the LV and/or RV. These segmentation maps are important for deriving clinical indices, such as left ventricular end-diastolic volume (LVEDV), left ventricular end-systolic volume (LVESV), right ventricular end-diastolic volume (RVEDV), right ventricular end-systolic volume (RVESV), and EF. In addition, these segmentation maps are essential for 3D shape analysis (Xue et al., 2018; Biffi et al., 2018), 3D+time motion analysis (Zheng et al., 2019) and survival prediction (Bello et al., 2019).

3.1 Cardiac MR Image Segmentation

Cardiac MRI is a non-invasive imaging technique that can visualize the structures within and around the heart. Compared to CT, it does not require ionising radiation. Instead, it relies on the magnetic

field in conjunction with radio-frequency waves to excite hydrogen nuclei in the heart, and then generates an image by measuring their response. By utilizing different imaging sequences, cardiac MRI allows accurate quantification of both cardiac anatomy and function (e.g. cine imaging) and pathological tissues such as scars (late gadolinium enhancement (LGE) imaging). Accordingly, cardiac MRI is currently regarded as the gold standard for quantitative cardiac analysis (Van Der Geest and Reiber, 1999).

A group of representative deep learning based cardiac MR segmentation methods are shown in Table 1. From the table, one can see that a majority of works have focused on segmenting cardiac chambers (e.g. LV, RV, LA). In contrast, there are relatively fewer works on segmenting abnormal cardiac tissue regions such as myocardial scars and atrial fibrosis. This is likely due to the limited relevant public datasets as well as the difficulty of the task. In addition, to the best of our knowledge, there are very few works that apply deep learning techniques to atrial wall segmentation, as also suggested by a recent survey paper (Karim et al., 2018). In the following sections, we will describe and discuss these methods regarding different applications in detail.

3.1.1 Ventricle Segmentation

Vanilla FCN-based Segmentation: Tran (2016) was among the first ones to apply a FCN (Shelhamer et al., 2017) to segment the left ventricle, myocardium and right ventricle directly on short-axis cardiac magnetic resonance (MR) images. Their end-to-end approach based on FCN achieved competitive segmentation performance, significantly outperforming traditional methods in terms of both speed and accuracy. In the following years, a number of works based on FCNs have been proposed, aiming at achieving further improvements in segmentation performance. In this regard, one stream of work focuses on optimizing the network structure to enhance the feature learning capacity for segmentation (Khened et al., 2019; Li et al., 2019b; Zhou and Yang,

Table 1. A summary of representative deep learning methods on cardiac MRI segmentation. SAX: short-axis view; 2CH: 2-chamber view; 4CH: 4-chamber view; ED: end-diastolic; ES: end-systolic.

Application	Selected works	Description	Type of Images	Structure(s)
Ventricle Segmentation	FCN-based			
	Tran (2016)	2D FCN	SAX	Bi-ventricle
	Lieman-Sifry et al. (2017)	A lightweight FCN (E-Net)	SAX	Bi-ventricle
	Isensee et al. (2017)	2D U-net +3D U-net (ensemble)	SAX	Bi-ventricle
	Jang et al. (2017)	2D M-Net with weighted cross entropy loss	SAX	Bi-ventricle
	Baumgartner et al. (2017)	2D U-net with cross entropy	SAX	Bi-ventricle
	Bai et al. (2018a)	2D FCN trained and verified on a large dataset (~ 5000 subjects);	SAX, 2CH, 4CH	Four chambers
	Tao et al. (2019)	2D U-net trained and verified on a multi-vendor, multi-scanner dataset	SAX	LV
	Khened et al. (2019)	2D Dense U-net with inception module	SAX	Bi-ventricle
	Fahmy et al. (2019)	2D FCN	SAX	LV
	Introducing spatial or temporal context			
	Poudel et al. (2016)	2D FCN with RNN to model inter-slice coherency	SAX	Bi-ventricle
	Patravali et al. (2017)	2D multi-channel FCN to aggregate inter-slice information	SAX	Bi-ventricle
	Wolterink et al. (2017c)	Dilated U-net to segment ED and ES simultaneously	SAX	Bi-ventricle
	Applying anatomical constraints			
	Oktay et al. (2018a)	FCN trained with additional anatomical shape-based regularization	SAX;US	LV
	Multi-stage networks			
	Tan et al. (2017)	Semi-automated method; CNN (localization) followed by another CNN to derive contour parameters	SAX	LV
	Zheng et al. (2018)	FCN (localization) + FCN (segmentation); Propagate labels from adjacent slices	SAX	Bi-ventricle
	Vigneault et al. (2018)	U-net (initial segmentation) + CNN (localization and transformation) + Cascaded U-net (segmentation)	SAX, 2CH, 4CH	Four chambers
Hybrid segmentation methods				
Avendi et al. (2016, 2017)	CNN (localization) +AE (shape initialization) + Deformable model	SAX	LV; RV	
Yang et al. (2016)	CNN combined with Multi-atlas	SAX	LV	
Ngo et al. (2017)	Level-set based segmentation with Deep belief networks	SAX	LV	
Atrial Segmentation	Mortazi et al. (2017b)	Multi-view CNN with adaptive fusion strategy	3D scans	LA
Xiong et al. (2019)	Patch-based dual-stream 2D FCN	LGE MRI	LA	
Xia et al. (2018)	Two-stage pipeline; 3D U-net (localization) +3D U-net (segmentation)	LGE MRI	LA	
Scar Segmentation	Yang et al. (2018b)	Fully automated; Multi-atlas method for LA segmentation followed by an AE to find the atrial scars	LGE MRI	LA; atrial scars
	Chen et al. (2018b)	Fully automated; Multi-view Two-Task Recursive Attention Model	LGE MRI	LA; atrial scars
	Zabihollahy et al. (2018)	Semi-automated; 2D CNN for scar tissue classification	LGE MRI	Myocardial scars
	Moccia et al. (2019)	Semi-automated; 2D FCN for scar segmentation	LGE MRI	Myocardial scars
	Xu et al. (2018a)	Fully automated; RNN for joint motion feature learning and scar segmentation	cine MRI	Myocardial scars
Aorta Segmentation	Bai et al. (2018b)	RNN to learn temporal coherence; Propagate labels from labeled frames to unlabeled adjacent frames for semi-supervised learning;	cine MRI	Aorta
Whole Heart Segmentation	Yu et al. (2017a)	3D U-net with deep supervision	3D scans	Blood pool+Myocardium of the heart
	Li et al. (2017)	3D FCN with deep supervision	3D scans	Blood pool+Myocardium of the heart
	Wolterink et al. (2017a)	dilated CNN with deep supervision	3D scans	Blood pool+Myocardium of the heart

2019; Zhang et al., 2019a; Cong and Zhang, 2018; Jang et al., 2017; Fahmy et al., 2019). For example, Khened et al. (2019) developed a dense U-net with inception modules to combine multi-scale features for robust segmentation across images with large anatomical variability. Jang et al. (2017); Yang et al. (2017c); Sander et al. (2019); Chen et al. (2019e) investigated different loss functions such as weighted cross-entropy, weighted Dice loss, deep supervision loss and focal loss to improve the segmentation performance. Among these FCN-based methods, the majority of approaches use 2D networks rather than 3D networks for segmentation. This is mainly due to the typical low through-plane resolution and motion artifacts of most cardiac MR scans, which limits the applicability of 3D networks (Baumgartner et al., 2017).

Introducing spatial or temporal context: One drawback of using 2D networks for cardiac segmentation is that these networks work slice by slice, and thus they do not leverage any inter-slice dependencies. As a result, 2D networks can fail to locate and segment the heart on challenging slices such as apical and basal slices where the contours of the ventricles are not well defined. To address this problem, a number of works have attempted to introduce additional contextual information to guide 2D FCN. This contextual information can include shape priors learned from labels or multi-view images (Zotti et al., 2017, 2019; Chen et al., 2019b). Others extract spatial information from adjacent slices to assist the segmentation, using recurrent units (RNNs) or multi-slice networks (2.5D networks) (Poudel et al., 2016; Patravali et al., 2017; Du et al., 2019; Zheng et al., 2018).

These networks can also be applied to leveraging information across different temporal frames in the cardiac cycle to improve spatial and temporal consistency of segmentation results (Yan et al., 2018; Savioli et al., 2018; Du et al., 2019; Qin et al., 2018a; Wolterink et al., 2017c).

Applying anatomical constraints: Another problem that may limit the segmentation performance of both 2D and 3D FCNs is that they are typically trained with pixel-wise loss functions only (e.g. cross-entropy or soft-Dice losses). These pixel-wise loss functions may not be sufficient to learn features that represent the underlying anatomical structures. Several approaches therefore focus on designing and applying anatomical constraints to train the network to improve its prediction accuracy and robustness. These constraints are represented as regularization terms which take into account the topology (Clough et al., 2019), contour and region information (Chen et al., 2019g) or shape information (Oktay et al., 2018a; Yue et al., 2019), encouraging the network to generate more anatomically plausible segmentations. In addition to regularizing networks at training time, Painchaud et al. (2019) proposed a variational AE to correct inaccurate segmentations, in the post-processing stage.

Multi-task learning: Multi-task learning has also been explored to regularize FCN-based cardiac ventricle segmentation during training by performing auxiliary tasks that are relevant to the main segmentation task, such as motion estimation (Qin et al., 2018b), estimation of cardiac function (Dangi et al., 2018b), ventricle size classification (Zhang et al., 2018b) and image reconstruction (Chartsias et al., 2018; Huang et al., 2019). Training a network for multiple tasks simultaneously encourages the network to extract features which are useful across these tasks, resulting in improved learning efficiency and prediction accuracy.

Multi-stage networks: Recently, there is a growing interest in applying neural networks in a multi-stage pipeline which breaks down the

segmentation problem into subtasks (Vigneault et al., 2018; Zheng et al., 2018; Li et al., 2019a; Tan et al., 2017; Liao et al., 2019). For example, Zheng et al. (2018); Li et al. (2019a) proposed a region-of-interest (ROI) localization network followed by a segmentation network. Likewise, Vigneault et al. (2018) proposed a network called Omega-Net which consists of a U-net for cardiac chamber localization, a learnable transformation module to normalize image orientation and a series of U-nets for fine-grained segmentation. By explicitly localizing the ROI and by rotating the input image into a canonical orientation, the proposed method better generalizes to images with varying sizes and orientations.

Hybrid segmentation methods: Another stream of work aims at combining neural networks with classical segmentation approaches, e.g. level-sets (Ngo et al., 2017; Duan et al., 2018a), deformable models (Avendi et al., 2016, 2017; Medley et al., 2019), atlas-based methods (Yang et al., 2016; Rohé et al., 2017) and graph-cut based methods (Lu et al., 2019). Here, neural networks are applied in the feature extraction and model initialization stages, reducing the dependency on manual interactions and improving the segmentation accuracy of the conventional segmentation methods deployed afterwards. For example, Avendi et al. (2016) proposed one of the first DL-based methods for LV segmentation in cardiac short-axis MR images. The authors first applied a CNN to automatically detect the LV and then used an AE to estimate the shape of the LV. The estimated shape was then used to initialize follow-up deformable models for shape refinement. As a result, the proposed integrated deformable model converges faster than conventional deformable models and the segmentation achieves higher accuracy. In their later work, the authors extended this approach to segment RV (Avendi et al., 2017). While these hybrid methods demonstrated better segmentation accuracy than previous non-deep learning methods, most of them still require an iterative optimization for shape refinement. Furthermore, these methods are often designed for one particular anatomical structure. As noted in

the recent benchmark study (Bernard et al., 2018), most state-of-the-art segmentation algorithms for bi-ventricle segmentation are based on end-to-end FCNs, which allows the simultaneous segmentation of the LV and RV.

To better illustrate these developments for cardiac ventricle segmentation from cardiac MR images, we collate a list of bi-ventricle segmentation methods that have been trained and tested on the Automated Cardiac Diagnosis Challenge (ACDC) dataset, reported in Table 2. For ease of comparison, we only consider those methods which have been evaluated on the same online test set (50 subjects). As the ACDC challenge organizers keep the online evaluation platform open to the public, our comparison not only includes the methods from the original challenge participants (summarized in the benchmark study paper from Bernard et al. (2018)) but also three segmentation algorithms that have been proposed after the challenge (i.e. Zotti et al. (2019); Li et al. (2019a); Painchaud et al. (2019)). From this comparison, one can see that top algorithms are the ensemble method proposed by Isensee et al. (2017) and the two-stage method proposed by Li et al. (2019a), both of which are based on FCNs. In particular, compared to the traditional level-set method (Tziritis and Grinias, 2017), both methods achieved considerably higher accuracy even for the more challenging segmentation of the left ventricular myocardium (Myo), indicating the power of deep learning based approaches.

3.1.2 Atrial Segmentation

Atrial fibrillation (AF) is one of the most common cardiac electrical disorders, affecting around 1 million people in the UK³. Accordingly, atrial segmentation is of prime importance in the clinic, improving the assessment of the atrial anatomy in both pre-operative atrial fibrillation (AF) ablation planning and post-operative follow-up evaluations. In addition, the segmentation of atrium can be used as a basis for scar segmentation and

atrial fibrosis quantification from LGE images. Traditional methods such as region growing (Karim et al., 2008) and methods that employ strong priors (i.e. atlas-based label fusion (Tao et al., 2016) and non-rigid registration (Zhuang et al., 2010)) have been applied in the past for automated left atrium segmentation. However, the accuracy of these methods highly relies on good initialization and ad-hoc pre-processing methods, which limits the widespread adoption in the clinic.

Recently, Bai et al. (2018a) and Vigneault et al. (2018) applied 2D FCNs to directly segment the LA and RA from standard 2D long-axis images, i.e. 2-chamber (2CH), 4-chamber (4CH) views. Notably, their networks can also be trained to segment ventricles from 2D short-axis stacks without any modifications to the network architecture. Likewise, Xiong et al. (2019); Preetha et al. (2018); Bian et al. (2018); Chen et al. (2018a) applied 2D FCNs to segment the atrium from 3D LGE images in a slice-by-slice fashion, where they optimized the network structure for enhanced feature learning. 3D networks (Xia et al., 2018; Savioli et al., 2018; Jia et al., 2018; Vesal et al., 2018; Li et al., 2018) and multi-view FCN (Mortazi et al., 2017b; Yang et al., 2018a) have also been explored to capture 3D global information from 3D LGE images for accurate atrium segmentation.

In particular, Xia et al. (2018) proposed a fully automatic two-stage segmentation framework which contains a first 3D U-net to roughly locate the atrial center from down-sampled images followed by a second 3D U-net to accurately segment the atrium in the cropped portions of the original images at full resolution. Their multi-stage approach is both memory-efficient and accurate, ranking first in the left atrium segmentation challenge 2018 (LASC'18) with a mean Dice score of 0.93 evaluated on a test set of 54 cases.

3.1.3 Scar Segmentation

Scar characterization is usually performed using LGE MR imaging, a contrast-enhanced MR imaging technique. LGE MR imaging enables the

³ <https://www.nhs.uk/conditions/atrial-fibrillation/>

Table 2. Segmentation accuracy of state-of-the-art segmentation methods verified on the cardiac bi-ventricular segmentation challenge (ACDC) dataset (Bernard et al., 2018) All the methods were evaluated on the same test set (50 subjects). Bold numbers are the highest overall Dice values for the corresponding structure. LV: left ventricle, RV: right ventricle, Myo: left ventricular myocardium; ED: end-diastolic; ES: end-systolic. Last update: 2019.8.1.

Methods	Description	LV	Myo	RV
Isensee et al. (2017)	2D U-net +3D U-net (ensemble)	0.950	0.911	0.923
Li et al. (2019a)	Two 2D FCNs for ROI detection and segmentation respectively;	0.944	0.911	0.926
Zotti et al. (2019)	2D GridNet-MD with registered shape prior	0.938	0.894	0.910
Khened et al. (2019)	2D Dense U-net with inception module	0.941	0.894	0.907
Baumgartner et al. (2017)	2D U-net with cross entropy loss	0.937	0.897	0.908
Zotti et al. (2017)	2D GridNet with registered shape prior	0.931	0.890	0.912
Jang et al. (2017)	2D M-Net with weighted cross entropy loss	0.940	0.885	0.907
Painchaud et al. (2019)	FCN followed by an AE for shape correction	0.936	0.889	0.909
Wolterink et al. (2017c)	Multi-input 2D dilated FCN, segmenting paired ED and ES frames simultaneously	0.940	0.885	0.900
Patravali et al. (2017)	2D U-net with a Dice loss	0.920	0.890	0.865
Rohé et al. (2017)	Multi-atlas based method combined with 3D CNN for registration	0.929	0.868	0.881
Tziritas and Grinias (2017)	Level-set +markov random field (MRF); <i>Non-deep learning method</i>	0.907	0.798	0.803
Yang et al. (2017c)	3D FCN with deep supervision	0.820	N/A	0.780

Note that for simplicity, we report the average Dice scores for each structure over ED and ES phases. More detailed comparison for different phases can be found on the public leaderboard in the post testing part (<https://acdc.creatis.insa-lyon.fr>) as well as corresponding published works in this table.

identification of myocardial scars and atrial fibrosis, allowing improved management of myocardial infarction and atrial fibrillation (Kim et al., 1999). Prior to the advent of deep learning, scar segmentation was often performed using intensity thresholding-based or clustering methods which are sensitive to the local intensity changes (Zabihollahy et al., 2018). The main limitation of these methods is that they usually require the manual segmentation of the region of interest to reduce the search space and the computational costs (Carminati et al., 2016). As a result, these semi-automated methods are not suitable for large-scale studies or clinical deployment.

Deep learning approaches have been combined with traditional segmentation methods for the purpose of scar segmentation: Yang et al. (2017a, 2018b) applied an atlas-based method to identify the left atrium and then applied deep neural networks to detect fibrotic tissue in that region. Relatively to end-to-end approaches, Chen et al. (2018b) applied deep neural networks to segment both the left atrium and the atrial scars. In particular, the authors employed a multi-view CNN with a recursive attention module to fuse features from complementary views for better segmentation accuracy. Their approach achieved a mean Dice score of 0.90 for the LA region and a mean Dice score of 0.78 for atrial scars.

In the work of Fahmy et al. (2018), the authors applied a U-net based network to segment the myocardium and the scars at the same time from LGE images acquired from patients with hypertrophic cardiomyopathy (HCM), achieving a fast segmentation speed. However, the reported segmentation accuracy for the scar regions was relatively low (mean Dice: 0.58). Zabihollahy et al. (2018); Moccia et al. (2019) instead adopted a semi-automated method which requires a manual segmentation of the myocardium followed by the application of a 2D network to differentiate scars from normal myocardium. They reported higher segmentation accuracy on their test sets (mean Dice >0.68). At the moment, fully-automated scar segmentation is still a challenging task since the infarcted regions in patients can lead to kinematic variabilities and abnormalities in those contrast-enhanced images. Interestingly, Xu et al. (2018a) developed an RNN which leverages motion patterns to automatically delineate myocardial infarction area from cine MR image sequences without contrast agents. Their method achieved a high overall Dice score of 0.90 when compared to the manual annotations on LGE MR images, providing a novel approach for infarction assessment.

3.1.4 Aorta Segmentation

The segmentation of the aortic lumen from cine MR images is essential for accurate mechanical

and hemodynamic characterization of the aorta. One common challenge for this task is the typical sparsity of the annotations in aortic cine image sequences, where only a few frames have been annotated. To address the problem, Bai et al. (2018b) applied a non-rigid image registration method (Rueckert et al., 1999) to propagate the labels from the annotated frames to the unlabeled neighboring ones in the cardiac cycle, effectively generating pseudo annotated frames that could be utilized for further training. This semi-supervised method achieved an average Dice metric of 0.96 for the ascending aorta and 0.95 for the descending aorta over a test set of 100 subjects. In addition, compared to a previous approach based on deformable models (Herment et al., 2010), their approach based on FCN and RNN can directly perform the segmentation task on a whole image sequence without requiring the explicit estimation of the ROI.

3.1.5 Whole Heart Segmentation

Apart from the above mentioned segmentation applications which target one particular structure, deep learning can also be used to segment the main substructures of the heart in 3D MR images (Yu et al., 2017a; Wolterink et al., 2017a; Li et al., 2017; Shi et al., 2018). An early work from Yu et al. (2017a) adopted a 3D dense FCN to segment the myocardium and blood pool in the heart from 3D MR scans. Recently, more and more methods began to apply deep learning pipelines to segment more specific substructures (incl. four chambers, myocardium (MYO), aorta, pulmonary vein (PV)) in both 3D CT and MR images. This has been facilitated by the availability of public datasets for whole heart segmentation (Multi-Modality Whole Heart Segmentation (MM-WHS)). In general, the segmentation task on MR images is harder than the one of CT images mainly because of the large variations in terms of image intensity distribution among different scanners. As mentioned in a recent benchmark study paper by Zhuang et al. (2019), deep learning methods in general achieve better segmentation accuracy on CT images compared

to that of MR images. We will discuss these segmentation methods in the next CT section in further detail (see section 3.2.1).

3.2 Cardiac CT Image Segmentation

CT is a non-invasive imaging technique that is performed routinely for disease diagnosis and treatment planning. In particular, cardiac CT scans are used for assessment of cardiac anatomy and specifically the coronary arteries. There are two main imaging modalities: non-contrast CT imaging and contrast-enhanced coronary CT angiography (CTA). Typically, non-contrast CT imaging exploits density of tissues to generate an image, such that different densities using various attenuation values such as soft tissues, calcium, fat, and air can be easily distinguished, and thus allows to estimate the amount of calcium present in the coronary arteries (Kang et al., 2012). In comparison, contrast-enhanced coronary CTA, which is acquired after the injection of a contrast agent, can provide excellent visualization of cardiac chambers, vessels and coronaries, and has been shown to be effective in detecting non-calcified coronary plaques. In the following sections, we will review some of the most commonly used deep learning-based cardiac CT segmentation methods. A summary of these approaches is presented in Table 3.

3.2.1 Cardiac Substructure Segmentation

Accurate delineation of cardiac substructures plays a crucial role in cardiac function analysis, providing important clinical variables such as EF, myocardial mass, wall thickness etc. Typically, the cardiac substructures that are segmented include the LV, RV, LA, RA, MYO, aorta (AO) and pulmonary artery (PA).

Two-step segmentation: One group of deep learning methods relies on a two-step segmentation procedure, where a ROI is first extracted and then fed into a CNN for subsequent classification (Zreik et al., 2016; Dormer et al., 2018). For instance, Zreik et al. (2016) proposed a two-step LV segmentation process where a bounding box for the LV is first detected using the method described

Table 3. A summary of selected deep learning methods on cardiac CT segmentation.

Application	Selected works	Description	Imaging Modality	Structure(s)
Cardiac Substructure Segmentation	Two-step segmentation			
	Zreik et al. (2016)	patch based CNN	CTA	LV
	Payer et al. (2018)	a pipeline of two FCNs	MR/CT	WHS
	Tong et al. (2017)	deeply supervised 3D U-net	MR/CT	WHS
	Wang et al. (2018)	two-stage 3D U-net with dynamic ROI extraction	MR/CT	WHS
	Xu et al. (2018b)	faster RCNN and U-net	CT	WHS
	Multi-view CNNs			
	Wang and Smedby (2017)	orthogonal 2D U-nets with shape context	MR/CT	WHS
	Mortazi et al. (2017a)	multi-planar FCNs with an adaptive fusion strategy	MR/CT	WHS
	Hybrid loss			
Yang et al. (2017d)	3D U-net with deep supervision	MR/CT	WHS	
Ye et al. (2019)	3D deeply-supervised U-net with multi-depth fusion	CT	WHS	
Others				
Zreik et al. (2018a)	multi-scale FCN	CTA	Myo	
Joyce et al. (2018)	unsupervised segmentation with GANs	MR/CT	LV/RV/Myo	
Coronary Artery Segmentation	End-to-end CNNs			
	Moeskops et al. (2016)	multi-task CNN	CTA	Vessel
	Merkow et al. (2016)	3D U-net with deep multi-scale supervision	CTA	Vessel
	Lee et al. (2019)	template transformer network	CTA	Vessel
	CNN as pre-/post-processing			
	Gülşin et al. (2016)	CNN as path pruning	CTA	coronary artery centerline
	Guo et al. (2019)	multi-task FCN with a minimal patch extractor	CTA	coronary artery centerline
	Shen et al. (2019)	3D FCN with level set	CTA	Vessel
	Others			
	Wolterink et al. (2019b)	CNN to estimate direction classification and radius regression	CTA	coronary artery centerline
Wolterink et al. (2019a)	graph convolutional network	CTA	Vessel	
Coronary Artery Calcium and Plaque Segmentation	Two-step segmentation			
	Wolterink et al. (2016)	CNN pairs	CTA	CAC
	Lessmann et al. (2016)	multi-view CNNs	CT	CAC
	Lessmann et al. (2017)	two consecutive CNNs	CT	CAC
	Liu et al. (2018)	3D vessel-focused ConvNets	CTA	CAC/NCF/MCP
	Direct segmentation			
	Santini et al. (2017)	patch based CNN	CT	CAC
	Shadmi et al. (2018)	U-net and FC DenseNet	CT	CAC
	Zhang et al. (2019c)	U-DenseNet	CT	CAC
	Ma and Zhang (2019)	DenseRAU-net	CT	CAC

in (de Vos et al., 2017), followed by a voxel classification within the defined bounding box using a patch-based CNN. More recently, FCN, especially U-net (Ronneberger and Brox, 2015), has become the method of choice for cardiac CT segmentation. Zhuang et al. (2019) provides a comparison of a group of methods (Payer et al., 2018; Wang and Smedby, 2017; Yang et al., 2017b,d; Tong et al., 2017; Mortazi et al., 2017a) for whole heart segmentation (WHS) that have been evaluated on the MM-WHS challenge. Several of these methods (Payer et al., 2018; Tong et al., 2017; Xu et al., 2018b; Wang et al., 2018) combine a localization network, which produces a coarse detection of the heart, with 3D FCNs applied to the detected ROI for segmentation. This allows the segmentation network to focus on the anatomically relevant regions, and has shown to be effective for whole heart segmentation. In the MM-WHS challenge the method of Payer et al. (2018) ranked 1st. A summary of the comparison between the segmentation accuracy of the methods evaluated on

MM-WHS dataset is presented in Table 4. For more details, please refer to Zhuang et al. (2019).

Multi-view CNNs: Another line of research utilizes the volumetric information of the heart by training multi-planar CNNs (axial, sagittal, and coronal views) in a 2D fashion. Examples include Wang and Smedby (2017) and Mortazi et al. (2017a) where three independent orthogonal CNNs were trained to segment different views. Specifically, Wang and Smedby (2017) additionally incorporated shape context in the framework for the segmentation refinement, while Mortazi et al. (2017a) adopted an adaptive fusion strategy to combine multiple outputs utilising complementary information from different planes.

Hybrid loss: Several methods employ a hybrid loss, where different loss functions (such as focal loss, Dice loss, and weighted categorical cross-entropy) are combined to address the class imbalance issue, e.g. the volume size imbalance among different ventricular structures, and to

Table 4. Segmentation accuracy of methods validated on MM-WHS dataset. The training set contains 20 CT and 20 MRI whereas the test set contains 40 CT and 40 MRI. Reported numbers are Dice scores (CT/MRI) for different substructures on both CT and MRI scans. For more detailed comparisons, please refer to Zhuang et al. (2019).

Methods	LV	RV	LA	RA	MYO	AO	PA	WHS
Payer et al. (2018)	91.8/91.6	90.9 /86.8	92.9/85.5	88.8 /88.1	88.1/77.8	93.3/88.8	84.0/73.1	90.8 /86.3
Yang et al. (2017b)	92.3/75.0	85.7/75.0	93.0 /82.6	87.1/85.9	85.6/65.8	89.4/80.9	83.5/72.6	89.0/78.3
Mortazi et al. (2017a)	90.4/87.1	88.3/83.0	91.6/81.1	83.6/75.9	85.1/74.7	90.7/83.9	78.4/71.5	87.9/81.8
Tong et al. (2017)	89.3/70.2	81.0/68.0	88.9/67.6	81.2/65.4	83.7/62.3	86.8/59.9	69.8/47.0	84.9/67.4
Wang et al. (2018)	80.0/86.3	78.6/84.9	90.4/85.2	79.4/84.0	72.9/74.4	87.4/82.4	64.8/78.8	80.6/83.2
Ye et al. (2019)	94.4 / -	89.5/ -	91.6/ -	87.8/ -	88.9 / -	96.7 / -	86.2 / -	90.7/ -
Xu et al. (2018b)	87.9/ -	90.2/ -	83.2/ -	84.4/ -	82.2/ -	91.3/ -	82.1/ -	85.9/ -

improve the segmentation performance (Yang et al., 2017d; Ye et al., 2019).

In addition, the work of Zreik et al. (2018a) has proposed a method for the automatic identification of patients with significant coronary artery stenoses through the segmentation and analysis of the LV myocardium. In this work, a multi-scale FCN is first employed for myocardium segmentation, and then a convolutional autoencoder is used to characterize the LV myocardium, followed by a support vector machine (SVM) to classify patients based on the extracted features.

3.2.2 Coronary Artery Segmentation

Quantitative analysis of coronary arteries is an important step for the diagnosis of cardiovascular diseases, stenosis grading, blood flow simulation and surgical planning (Zhang, 2010). Though this topic has been studied for years (Lesage et al., 2009), only a small number of works investigate the use of deep learning in this context. Methods relating to coronary artery segmentation can be mainly divided into two categories: centerline extraction and lumen (i.e. vessel wall) segmentation.

CNNs as a post-/pre-processing step: Coronary centerline extraction is a challenging task due to the presence of nearby cardiac structures and coronary veins as well as motion artifacts in cardiac CT. Several deep learning approaches employ CNNs as either a post-processing or pre-processing step for traditional methods. For instance, Gülsün et al. (2016) formulated centerline extraction as

finding the maximum flow paths in a steady state porous media flow, with a learning-based classifier estimating anisotropic vessel orientation tensors for flow computation. A CNN classifier was then employed to distinguish true coronary centerlines from leaks into non-coronary structures. Guo et al. (2019) proposed a multi-task FCN centerline extraction method that can generate a single-pixel-wide centerline, where the FCN simultaneously predicted centerline distance maps and endpoint confidence maps from coronary arteries and ascending aorta segmentation masks, which were then used as input to the subsequent minimal path extractor to obtain the final centerline extraction results. In contrast, unlike the aforementioned methods that used CNNs either as a pre-processing or post-processing step, Wolterink et al. (2019b) proposed to address centerline extraction via a 3D dilated CNN, where the CNN was trained on patches to directly determine a posterior probability distribution over a discrete set of possible directions as well as to estimate the radius of an artery at the given point.

End-to-end CNNs: With respect to the lumen or vessel wall segmentation, most deep learning based approaches use an end-to-end CNN segmentation scheme to predict dense segmentation probability maps (Moeskops et al., 2016; Merkow et al., 2016; Huang et al., 2018; Shen et al., 2019). In particular, Moeskops et al. (2016) proposed a multi-task segmentation framework where a single CNN can be trained to perform three different tasks including coronary artery segmentation in cardiac CTA and tissue segmentation in brain

MR images. They showed that such a multi-task segmentation network in multiple modalities can achieve equivalent performance as a single task network. Merkow et al. (2016) introduced deep multi-scale supervision into a 3D U-net architecture, enabling efficient multi-scale feature learning and precise voxel-level predictions. Besides, shape priors can also be incorporated into the network (Lee et al., 2019; Chen et al., 2019h; Duan et al., 2018b). For instance, Lee et al. (2019) explicitly enforced a roughly tubular shape prior for the vessel segments by introducing a template transformer network, through which a shape template can be deformed via network-based registration to produce an accurate segmentation of the input image, as well as to guarantee topological constraints. More recently, graph convolutional networks have also been investigated by Wolterink et al. (2019a) for coronary artery segmentation in CTA, where vertices on the coronary lumen surface mesh were considered as graph nodes and the locations of these tubular surface mesh vertices were directly optimized. They showed that such method significantly outperformed a baseline network that used only fully-connected layers on healthy subjects (mean Dice score: 0.75 vs 0.67). Besides, the graph convolutional network used in their work is able to directly generate smooth surface meshes without post-processing steps.

3.2.3 Coronary Artery Calcium and Plaque Segmentation

Coronary artery calcium (CAC) is a direct risk factor for cardiovascular disease. Clinically, CAC is quantified using the Agatston score (Agatston et al., 1990) which considers the lesion area and the weighted maximum density of the lesion (de Vos et al., 2019). Precise detection and segmentation of CAC are thus important for the accurate prediction of the Agatston score and disease diagnosis.

Two-step segmentation: One group of deep learning approaches to segmentation and automatic calcium scoring proposed to use a two-step segmentation scheme. For example, Wolterink et al. (2016) attempted to classify CAC in cardiac CTA

using a pair of CNNs, where the first CNN coarsely identified voxels likely to be CAC within a ROI detected using (de Vos et al., 2017) and then the second CNN further distinguished between CAC and CAC-like negatives more accurately. Similar to such a two-stage scheme, Lessmann et al. (2016, 2017) proposed to identify CAC in low-dose chest CT, in which a ROI of the heart or potential calcifications were first localized followed by a CAC classification process.

Direct segmentation: More recently, several approaches (Shadmi et al., 2018; Santini et al., 2017; Ma and Zhang, 2019; Zhang et al., 2019c) have been proposed for the direct segmentation of CAC from non-contrast cardiac CT or chest CT: the majority of them employed combinations of U-net (Ronneberger and Brox, 2015) and DenseNet (Huang et al., 2017) for precise quantification of CAC which showed that a sensitivity over 90% can be achieved Santini et al. (2017). These aforementioned approaches all follow the same workflow where the CAC is first identified and then quantified. An alternative approach is to circumvent the intermediate segmentation and to perform direct quantification, such as in (Cano-Espinosa et al., 2018; de Vos et al., 2019), which have proven that this approach is effective and promising.

Finally, for non-calcified plaque (NCP) and mixed-calcified plaque (MCP) in coronary arteries, only a limited number of works have been reported that investigate deep learning methods for segmentation and quantification (Zreik et al., 2018b; Liu et al., 2018). Yet, this is a very important task from a clinical point of view, since these plaques can potentially rupture and obstruct an artery, causing ischemic events and severe cardiac damage. In contrast to CAC segmentation, NCP and MCP segmentation are more challenging due to their similar appearances and intensities as adjacent tissues. Therefore, robust and accurate analysis often requires the generation of multi-planar reformatted (MPR) images that have been straightened along the centreline of the vessel. Recently, Liu et al. (2018) proposed a vessel-focused 3D convolutional network with attention

layers to segment three types of plaques on the extracted and reformatted coronary MPR volumes. Zreik et al. (2018b) presented an automatic method for detection and characterization of coronary artery plaques as well as determination of coronary artery stenosis significance, in which a multi-task convolutional RNN was used to perform both plaque and stenosis classification by analyzing the features extracted along the coronary artery in an MPR image.

3.3 Cardiac Ultrasound Image Segmentation

Cardiac ultrasound (US) imaging, also known as echocardiography, is an indispensable clinical tool for the assessment of cardiovascular function. It is often used clinically as the first imaging examination owing to its portability, low cost and real-time capability. While a number of traditional methods such as active contours, level-sets and active shape models have been employed to automate the segmentation of anatomical structures in ultrasound images (Noble and Boukerroui, 2006), the achieved accuracy is limited by various problems of ultrasound imaging such as low signal-to-noise ratio, varying speckle noise, low image contrast (especially between the myocardium and the blood pool), edge dropout and shadows cast by structures such as dense muscle and ribs.

As in cardiac MR and CT, several DL-based methods have been recently proposed to improve the performance of cardiac ultrasound image segmentation in terms of both accuracy and speed. The majority of these DL-based approaches focus on LV segmentation, with only few addressing the problem of aortic valve and LA segmentation. A summary of the reviewed works can be found in Table 5.

3.3.1 2D LV segmentation

Deep learning combined with deformable models: The imaging quality of echocardiography makes voxel-wise tissue classification highly challenging. To address this challenge, deep learning has been combined with deformable model

for LV segmentation in 2D images (Carneiro et al., 2010, 2012; Carneiro and Nascimento, 2010, 2013; Nascimento and Carneiro, 2014, 2019; Veni et al., 2018). Features extracted by trained deep neural networks were used instead of handcrafted features to improve accuracy and robustness.

Several works applied deep learning in a two-stage pipeline which first localizes the target ROI via rigid transformation of a bounding box, then segments the target structure within the ROI. This two-stage pipeline reduces the search region of the segmentation and increases robustness of the overall segmentation framework. Carneiro et al. (2010, 2012) first adopted this DL framework to segment the LV in apical long-axis echocardiograms. The method uses DBN (Hinton and Salakhutdinov, 2006) to predict the rigid transformation parameters for localization and the deformable model parameters for segmentation. The results demonstrated the robustness of DBN-based feature extraction to image appearance variations. Nascimento and Carneiro (2017) further reduced the training and inference complexity of the DBN-based framework by using sparse manifold learning in the rigid detection step.

To further reduce the computational complexity, some works perform segmentation in one step without resorting to the two-stage approach. Nascimento and Carneiro (2014, 2019) applied sparse manifold learning in segmentation, showing a reduced training and search complexity compared to their previous version of the method, while maintaining the same level of segmentation accuracy. Veni et al. (2018) applied a FCN to produce coarse segmentation masks, which is then further refined by a level-set based method.

Utilizing temporal coherence: Cardiac ultrasound data is often recorded as a temporal sequence of images. Several approaches aim to leverage the coherence between temporally close frames to improve the accuracy and robustness of the LV segmentation. Carneiro and Nascimento (2010, 2013) proposed a dynamic modeling method based on a sequential monte carlo (SMC) (or particle

Table 5. A summary of reviewed deep learning methods for US image segmentation. A[X]C is short for Apical [X]-chamber view. PLAX/PSAX: parasternal long-axis/short-axis. CETUS: using the dataset from Challenge on Endocardial Three-dimensional Ultrasound Segmentation.

Application	Selected works	Method	Structure	Imaging modality
2D LV	Combined with deformable models			
	Carneiro et al. (2010, 2012)	DBN with two-step approach: localization and fine segmentation	LV	2D A2C, A4C
	Nascimento and Carneiro (2017)	deep belief networks (DBN) and sparse manifold learning for the localization step	LV	2D A2C, A4C
	Nascimento and Carneiro (2014, 2019)	DBN and sparse manifold learning for one-step segmentation	LV	2D A2C, A4C
	Veni et al. (2018)	FCN (U-net) followed by level-set based deformable model	LV	2D A4C
	Utilizing temporal coherence			
	Carneiro and Nascimento (2010, 2013)	DBN and particle filtering for dynamic modeling	LV	2D A2C, A4C
	Jafari et al. (2018)	U-net and LSTM with additional optical flow input	LV	2D A4C
	Utilizing unlabeled data			
	Carneiro and Nascimento (2011, 2012)	DBN on-line retrain using external classifier as additional supervision	LV	2D A2C, A4C
	Smistad et al. (2017)	U-Net trained using labels generated by a Kalman filter based method	LV and LA	2D A2C, A4C
	Yu et al. (2017b)	Dynamic CNN fine-tuning with mitral valve tracking to separate LV from LA	Fetal LV	2D
Jafari et al. (2019)	U-net with TL-net (Girdhar et al., 2016) based shape constraint on unannotated frames	LV	2D A4C	
Utilizing data from multiple domains				
Chen et al. (2016)	FCN trained using annotated data of multiple anatomical structures	Fetal head and LV	2D head, A2-5C	
Trained directly on large datasets				
Smistad et al. (2018)	Real time CNN view-classification and segmentation	LV	2D A2C, A4C	
Leclerc et al. (2018)	U-net trained on a large heterogeneous dataset	LV	2D A4C	
3D LV	Dong et al. (2018a)	CNN for 2D coarse segmentation refined by 3D snake model	LV	3D (CETUS)
	Oktay et al. (2018a)	U-net with TL-net based shape constraint	LV	3D (CETUS)
	Dong et al. (2018b)	Atlas-based segmentation using DL registration and adversarial training	LV	3D
Others	Ghesu et al. (2016)	Marginal space learning and adaptive sparse neural network	Aortic valves	3D
	Degel et al. (2018)	V-net with TL-net based shape constraint and GAN-based domain adaptation	LA	3D
	Zhang et al. (2018a)	CNN for view-classification, segmentation and disease detection	Multi-chamber	2D PLAX, PSAX, A2-4C

filtering) framework with a transition model, in which the segmentation of the current cardiac phase depends on previous phases. The results show that this approach performs better than the previous method (Carneiro et al., 2010) which does not take temporal information into account. In a more recent work, Jafari et al. (2018) combined U-net, long-short term memory (LSTM) and inter-frame optical flow to utilize multiple frames for segmenting one target frame, demonstrating improvement in overall segmentation accuracy. The method was also shown to be more robust to image quality variations in a sequence than single-frame U-net.

Utilizing unlabeled data: Several works proposed to use non-DL based segmentation algorithms to help generating labels on unlabeled images, effectively increasing the amount of training data. To achieve this, Carneiro and Nascimento (2011, 2012) proposed on-line retraining strategies where segmentation network (DBN) is firstly initialized using a small set of labeled data and then applied to non-labeled data to propose annotations. The proposed annotations are then checked by external classifiers before being used to re-train the network. Smistad et al. (2017) trained a U-net using images annotated by a Kalman filtering based method (Smistad and Lindseth, 2014) and illustrated the potential of

using this strategy for pre-training. Alternatively, some works proposed to exploit unlabeled data without using additional segmentation algorithm. Yu et al. (2017b) proposed to train a CNN on a partially labeled dataset of multiple sequences, then fine-tuned the network for each individual sequence using manual segmentation of the first frame as well as CNN-produced label of other frames. Jafari et al. (2019) proposed a semi-supervised framework which enables training on both the labeled and unlabeled images. The framework uses an additional generative network, which is trained to generate ultrasound images from segmentation masks, as additional supervision for the unlabeled frames in the sequences. The generative network forces the segmentation network to predict segmentation that can be used to successfully generate the input ultrasound image.

Utilizing data from multiple domains: Apart from exploiting unlabeled data in the same domain, leveraging manually annotated data from multiple domains (e.g. different 2D ultrasound views with various anatomical structures) can also help to improve the segmentation in one particular domain. Chen et al. (2016) proposed a novel FCN-based network to utilize multi-domain data to learn generic feature representations. Combined with an iterative refinement scheme, the method

has shown superior performance in detection and segmentation over traditional database-guided method (Georgescu et al., 2005), FCN trained on single-domain and other multi-domain training strategies.

DL networks trained directly on large datasets:

The potential of CNN in segmentation has motivated the collection and labeling of large-scale datasets. Several methods have since shown that deep learning methods, most notably CNN-based methods, are capable of performing accurate segmentation directly without complex post-processing. Leclerc et al. (2018) performed a study to investigate the effect of the size of annotated data for the segmentation of the LV in 2D ultrasound images using a simple U-net. The authors demonstrated that the U-net approach significantly benefits from larger amounts of training data. Furthermore, Smistad et al. (2018) demonstrated the efficiency of CNN-based methods by successfully performing real-time view-classification and segmentation.

3.3.2 3D LV segmentation

Segmenting cardiac structures in 3D ultrasound is even more challenging than 2D. While having the potential to derive more accurate volume-related clinical indices, 3D echocardiograms suffer from lower temporal resolution and lower image quality compared to 2D echocardiograms. Moreover, 3D images dramatically increase the dimension of parameter space of neural networks, which poses computational challenges for deep learning methods.

One way to reduce the computational cost is to avoid direct processing of 3D data in deep learning networks. Dong et al. (2018a) proposed a two-stage method by first applying a 2D CNN to produce coarse segmentation maps on 2D slices from a 3D volume. The coarse 2D segmentation maps are used to initialize a 3D shape model which is then refined by 3D deformable model method (Kass et al., 1988). In addition, the authors used transfer learning to side-step the limited training data problem by

pre-training network on a large natural image segmentation dataset and then fine-tuning to the LV segmentation task.

Anatomical shape priors have been utilized to increase the robustness of deep learning-based segmentation methods to challenging 3D ultrasound images. Oktay et al. (2018a) proposed an anatomically constrained network where a shape constraint-based loss is introduced to train a 3D segmentation network. The shape constraint is based on the shape prior learned from segmentation maps using auto-encoders (Girdhar et al., 2016). Dong et al. (2018b) utilized shape prior more explicitly by combining a neural network with a conventional atlas-based segmentation framework. Adversarial training was also applied to encourage the method to produce more anatomically plausible segmentation maps, which contributes to its superior segmentation performance comparing to a standard voxel-wise classification 3D segmentation network (Milletari et al., 2016).

3.3.3 Left-atrium segmentation

Degel et al. (2018) adopted the aforementioned anatomical constrain in 3D LA segmentation to tackle the domain shift problem caused by variation of imaging device, protocol and patient condition. In addition to the anatomically constraining network, the authors applied an adversarial training scheme (Kamnitsas et al., 2017b) to improve the generalizability of the model to unseen domain.

3.3.4 Multi-chamber segmentation

Apart from LV segmentation, a few works (Zhang et al., 2018a; Smistad et al., 2017; Leclerc et al., 2019) applied deep learning methods to perform multi-chamber (including LV and LA) segmentation. In particular, Zhang et al. (2018a) demonstrated the applicability of CNNs on three tasks: view classification, multi-chamber segmentation and detection of cardiovascular diseases. Comprehensive validation on a large (non-public) clinical dataset showed that clinical metrics derived from automatic segmentation are comparable or superior than

manual segmentation. To resemble real clinical situations and thus encourages the development and evaluation of robust and clinically effective segmentation methods, a large-scale dataset for 2D cardiac ultrasound has been recently made public (Leclerc et al., 2019). The dataset and evaluation platform were released following the preliminary data requirement investigation of deep learning methods (Leclerc et al., 2018). The dataset is composed of apical 4-chamber view images annotated for LV and LA segmentation, with uneven imaging quality from 500 patients with varying conditions. Notably, the initial benchmarking (Leclerc et al., 2019) on this dataset has shown that modern encoder-decoder CNNs resulted in lower error than inter-observer error between human cardiologists.

3.3.5 Aortic valve segmentation

Ghesu et al. (2016) proposed a framework based on marginal space learning (MSL), deep neural networks (DNNs) and active shape model (ASM) to segment the aortic valve in 3D cardiac ultrasound volumes. An adaptive sparsely-connected neural network with reduced number of parameters is used to predict a bounding box to locate the target structure, where the learning of the bounding box parameters is marginalized into sub-spaces to reduce computational complexity. This framework showed significant improvement over the previous non-DL MSL (Zheng et al., 2008) method while achieving competitive run-time.

3.4 Discussion

So far, we have presented and discussed recent progress of deep learning-based segmentation methods in the three modalities (i.e. MR, CT, US) that are commonly used in the assessment of cardiovascular disease. To summarize, current state-of-the-art segmentation methods are mainly based on CNNs that employ the FCN or U-net architecture. In addition, there are several commonalities in the FCN-based methods for cardiac segmentation which can be categorized into four groups: 1) enhancing network feature

learning by employing advanced building blocks in networks (e.g. inception module, dilated convolutions), most of which have been mentioned earlier (Sec. 2.1.5); 2) alleviating the problem of class imbalance with advanced loss functions (e.g. weighted loss functions); 3) improving the networks' generalization ability and robustness through a multi-stage pipeline, multi-task learning, or multi-view feature fusion; 4) forcing the network to generate more anatomically-plausible segmentation results by incorporating shape priors, applying adversarial loss or anatomical constraints to regularize the network during training. It is also worthwhile to highlight that for cardiac image sequence segmentation (e.g. cine MR images, 2D US sequences), leveraging spatial and temporal coherence from these sequences with advanced neural networks (e.g. RNN (Bai et al., 2018b; Jafari et al., 2018), multi-slice FCN (Zheng et al., 2018)) has been explored and shown to be beneficial for improving the segmentation accuracy and temporal consistency of the segmentation maps.

While the results reported in the literature show that neural networks have become more sophisticated and powerful, it is also clear that performance has improved with the increase of publicly available training subjects. A number of DL-based methods (especially in MRI) have been trained and tested on public challenge datasets, which not only provide large amounts of data to exploit the capabilities of deep learning in this domain, but also a platform for transparent evaluation and comparison. In addition, many of the participants in these challenges have shared their code with other researchers via open-source community websites (e.g. Github). Transparent and fair benchmarking and sharing of code are both essential for continued progress in this domain. We summarize the existing public datasets in Table 6 and public code repositories in Table 7 for reference.

2D Networks vs 3D Networks: An interesting conclusion supported by Table 7 is that the target image type can affect the choice of network structures (i.e. 2D networks, 3D networks). For 3D imaging acquisitions such as LGE-MRI and

Table 6. Summary of public datasets on cardiac segmentation for the three modalities. Mostly are from the International Conference on Medical Image Computing and Computer-assisted Intervention (MICCAI) society.

Dataset Name/Reference	Year	Main modalities	#	Target(s)	Main Pathology
York (Andreopoulos and Tsotsos, 2008)	2008	cine MRI	33	LV	cardiomyopathy, aortic regurgitation, enlarged ventricles and ischemia
Sunnybrook (Radau and Others, 2009)	2009	cine MRI	45	LV	hypertrophy, heart failure w./w.o infarction
LVSC (Suinesiaputra et al., 2014)	2011	cine MRI	200	LV	coronary artery disease, myocardial infarction, myocarditis, ischaemic cardiomyopathy,
RVSC (Petitjean et al., 2015)	2012	cine MRI	48	RV	suspicion of arrhythmogenic, right ventricular dysplasia, dilated cardiomyopathy, hypertrophic cardiomyopathy, aortic stenosis
cDEMIRIS (Karim et al., 2013)	2012	LGE MRI	60	LA fibrosis and scar	atrial fibrillation
LVIC (Karim et al., 2016)	2012	LGE MRI	30	Myocardial scars	ischaemic cardiomyopathy
LASC'13 (Tobon-Gomez et al., 2015)	2013	3D MRI	30	LA	N/A
HVSMR (Pace et al., 2015)	2016	3D MRI	4	Blood pool, MYO	congenital heart defects
ACDC (Bernard et al., 2018)	2017	MRI	150	LV; RV	myocardial infarction, dilated/hypertrophic cardiomyopathy, abnormal RV
LASC'18 (Zhao, 2018)	2018	LGE MRI	150	LA	atrial fibrillation
MM-WHS (Zhuang et al., 2019)	2017	CT/MRI	60/60	WHS	myocardium infarction, atrial fibrillation, tricuspid regurgitation, aortic valve stenosis, Alagille syndrome, Williams syndrome, dilated cardiomyopathy, aortic coarctation, Tetralogy of Fallot
CAT08 (Schaap et al., 2009)	2008	CTA	32	Coronary artery centerline	Patients with presence of calcium scored as absent, modest or severe.
CLS12 (Kirişli et al., 2013)	2012	CTA	48	Coronary lumen and stenosis	Patients with different levels of coronary artery stenoses.
CETUS (Bernard et al., 2016)	2014	3D US	45	LV	myocardial infarction, dilated cardiomyopathy
CAMUS (Leclerc et al., 2019)	2019	2D US	500	LV, LA	Patients with EF < 45%

Table 7. Public code for DL-based cardiac image segmentation. SAX: short-axis view; WHS: whole heart segmentation.

Modality	Application(s)	Authors	Basic Network	Code Repo (If not specified, the repository is located under github.com)
MR (SAX)	Bi-ventricular Segmentation	Tran (2016)	2D FCN	vuptran/cardiac-segmentation
MR (SAX)	Bi-ventricular Segmentation	Baumgartner et al. (2017)	2D/3D U-net	baumgach/acdc_segmenter
MR (SAX)	Bi-ventricular Segmentation: 1st rank in ACDC challenge	Isensee et al. (2017)	2D+3D U-net (ensemble)	MIC-DKFZ/ACDC2017
MR (SAX)	Bi-ventricular Segmentation	Zheng et al. (2018)	cascaded 2D U-net	julien-zheng/CardiacSegmentationPropagation
MR (SAX)	Bi-ventricular segmentation and Motion Estimation	Qin et al. (2018a)	2D FCN, RNN	cq615
MR (SAX)	Biventricular Segmentation	Khened et al. (2019)	2D U-net	mahendrakhened
MR (3D scans)	Blood pool+MYO Segmentation	Yu et al. (2017a)	3D CNN	yulequan/HeartSeg
MR (Multi-view)	Four-chamber Segmentation and Aorta Segmentation	Bai et al. (2018a,b)	2D FCN, RNN	baiwenjia/ukbb_cardiac
MR	Cardiac Segmentation and Motion Tracking	Duan et al. (2019)	2.5D FCN +Atlas-based	j-duan/4Dsegment
LGE MRI	Left Atrial Segmentation	Chen et al. (2018a)	2D U-net	cherise215/atria_segmentation_2018
LGE MRI	Left Atrial Segmentation	Yu et al. (2019)	3D V-net	yulequan/UA-MI
CT	WHS	Yang et al. (2017d)	3D U-net	xy0806/miccai17-mmwhs-hybrid
CT	WHS	Xu et al. (2018b)	Faster RCNN, 3D U-net	Wuziyi616/CFUN
CT, MRI	Coronary arteries	Merkow et al. (2016)	3D U-net	jmerkow/I2I
CT, MRI	WHS	Dou et al. (2018, 2019)	2D CNN	carrenD/Medical-Cross-Modality-Domain-Adaptation
CT, MRI	WHS	Chen et al. (2019c)	2D CNN	cchen-cc/SIFA
US	View Classification and Four-chamber Segmentation	Zhang et al. (2018a)	2D U-net	bitbucket.org/rahuldeo/echocv

CT images, 3D networks are preferred whereas 2D networks are more popular approaches for segmenting cardiac cine short-axis or long-axis image stacks. One reason for using 2D networks for the segmentation of short-axis or long-axis images is their typically large slice thickness (usually around 7–8 mm) which can further exacerbated by inter-slice gaps. In addition, breath-hold related motion artifacts between different slices may negatively affect 3D networks. A study conducted by Baumgartner et al. (2017) has shown that a 3D U-net performs worse than a 2D U-net when evaluated on the ACDC challenge dataset. By contrast, in the LASC'18 challenge mentioned in Table 6, which uses high-resolution 3D images, most participants applied 3D networks and the best performance was achieved by a cascaded network based on the 3D U-net (Xia et al., 2018).

It is well known that training 3D networks is more difficult than training 2D networks. In general, 3D networks have significantly more parameters than 2D networks. Therefore, 3D networks are more difficult and computationally expensive to optimize as well as prone to over-fitting, especially if the training data is limited. As a result, several researchers have tried to carefully design the structure of network to reduce the number of parameters for a particular application and have also applied advanced techniques (e.g. deep supervision) to alleviate the over-fitting problem (Yu et al., 2017a; Xia et al., 2018). For this reason, 2D-based networks (e.g. 2D U-net) are still the most popular segmentation approaches for all three modalities.

In addition to 2D and 3D networks, several authors have proposed '2D+' networks that have been shown to be effective in segmenting structures from cardiac volumetric data. These

‘2D+’ networks are mainly based on 2D networks, but are adapted with increased capacity to utilize 3D context. These networks include multi-view networks which leverage multi-planar information (i.e. coronal, sagittal, axial views) (Mortazi et al., 2017b; Wang and Smedby, 2017), multi-slice networks, and 2D FCNs combined with RNNs which incorporate context across multiple slices (Duan et al., 2019; Patravali et al., 2017; Poudel et al., 2016; Du et al., 2019). These ‘2D+’ networks inherit the advantages of 2D networks while still being capable of leveraging through-plane spatial context for more robust segmentation with strong 3D consistency.

4 CHALLENGES AND FUTURE WORK

It is evident from the literature that deep learning methods have matched or surpassed the previous state of the art in a various cardiac segmentation applications, mainly benefiting from the increased size of public datasets and the emergence of advanced network architectures as well as powerful hardware for computing. Given this rapid process, one may wonder if deep learning methods can be directly deployed to real-world applications to reduce the workload of clinicians. The current literature suggests that there is still a long way to go. In the following paragraphs, we summarize several major challenges in the field of cardiac segmentation and some recently proposed approaches that attempt to address them. These challenges and related works also provide potential research directions for future work in this field.

4.1 Scarcity of Labels

One of the biggest challenges for deep learning approaches is the scarcity of annotated data. In this review, we found that the majority of studies uses a fully supervised approach to train their networks, which requires a large number of annotated images. In fact, annotating cardiac images is time consuming and often requires significant amounts of expertise. While data augmentation techniques such as cropping,

padding, and geometric transformations (e.g. affine transformations) can be used to increase the size of training samples, their diversity may still be limited, failing to reflect the spectrum of real-world data distributions. Several methods have been proposed to overcome this challenge. These methods can be categorized into four classes: transfer learning with fine-tuning, weakly and semi-supervised learning, self-supervised learning, and unsupervised learning.

- **Transfer learning with fine-tuning.** Transfer learning aims at reusing a model pre-trained on one task as a starting point to train for a second task. The key of transfer learning is to learn features in the first task that are related to the second task such that the network can quickly converge even with limited data. Several researchers have successfully demonstrated the use of transfer learning to improve the model generalization ability for cardiac ventricle segmentation across different scanners, where they first trained a model on a large dataset and then fine-tuned it on a small dataset (Bai et al., 2018a; Khened et al., 2019; Cong and Zhang, 2018; Fahmy et al., 2019; Chen et al., 2019f).
- **Weakly and semi-supervised learning.** Weakly and semi-supervised learning methods aim at improving the learning accuracy by making use of both labeled and unlabeled or weakly-labeled data (e.g. annotations in forms of scribbles or bounding boxes). In this context, several works have been proposed for cardiac ventricle segmentation in MR images. One approach is to estimate full labels on unlabeled or weakly labeled images for further training. For example, Bai et al. (2018b); Qin et al. (2018a) utilized motion information to propagate labels from labeled frames to unlabeled frames in a cardiac cycle whereas Bai et al. (2017); Can et al. (2018) applied the expectation maximization (EM) algorithm to predict and refine the estimated labels recursively. Others have explored different approaches to regularize the network when

training on unlabeled images, applying multi-task learning (Chartsias et al., 2018), or global constraints (Kervadec et al., 2019).

- **Self-supervised learning.** Another approach is self-supervised learning which aims at utilizing labels that are *generated automatically* without human intervention. These labels, designed to encode some properties or semantics of the object, can provide strong supervisory signals to pre-train a network before fine-tuning for a given task. A very recent work from Bai et al. (2019) has shown the effectiveness of self-supervised learning for cardiac MR image segmentation where the authors used auto-generated anatomical position labels to pre-train a segmentation network. Compared to a network trained from scratch, networks pre-trained on the self-supervised task performed better, especially when the training data was extremely limited.
- **Unsupervised learning.** Unsupervised learning aims at learning without paired labeled data. Compared to the former three classes, there is limited literature about unsupervised learning methods for cardiac image segmentation, perhaps because of the difficulty of the task. An early attempt has been made which applied adversarial training to train a network segmenting LV and RV from CT and MR images without requiring a training set of paired images and labels (Joyce et al., 2018).

Apart from utilizing unlabeled images for training neural networks, another interesting direction is active learning (Mahapatra et al., 2018), which tries to select the most representative images from a large-scale dataset, reducing redundant labeling workload and training cost. This technique is also related to incremental learning, which aims to improve the model performance with new classes added incrementally while avoiding a dramatic decrease in overall performance (Castro et al., 2018). Given the increasing size of the available medical datasets, and the practical challenges of labeling and storing large amounts of images

from various sources, it is of great interest to develop algorithms capable of distilling a large-scale cardiac dataset into a small one containing the most representative cases for labeling and training.

4.2 Model Generalization Across Various Imaging Modalities, Scanners and Pathologies.

Another common limitation in DL-based methods is that they still lack generalization capabilities when presented with previously unseen samples (e.g. data from a new scanner, abnormal and pathological cases that have not been included in the training set). In other words, deep learning models tend to be biased by their respective training datasets. This limitation prevents models to be deployed in the real world and therefore diminishes their impact for improving clinical workflows. To improve the model performance across MR images acquired from multiple vendors and multiple scanners, Tao et al. (2019) collected a large multi-vendor, multi-center, heterogeneous labeled training set from patients with cardiovascular diseases. However, this approach may not scale to the real world, as it implies the collection of a vastly large dataset covering all possible cases. Moreover, it still faces the aforementioned collecting and labeling challenge.

Unsupervised domain adaptation. Several researchers have recently started to investigate the use of unsupervised domain adaptation techniques that aim at optimizing the model performance on unseen datasets without additional labeling costs. Several works have successfully applied adversarial training for cross-modality segmentation tasks, adapting a cardiac segmentation model learned from MR images to CT images and vice versa (Dou et al., 2018, 2019; Ouyang et al., 2019; Chen et al., 2019c). These type of approaches can also be adopted for semi-supervised learning, where the target domain is a new set of unlabeled data of the same modality (Chen et al., 2019d).

Data augmentation. An alternative yet simple and effective approach is data augmentation. The

main idea is to increase the variety of training images so that the training set distribution is more close to the one of a test set in the real world. In general, this type of augmentation is achieved by applying a stack of geometric or photometric transformations to existing image-label pairs. Recently, Chen et al. (2019a) have proposed a data normalization and augmentation pipeline which enables a neural network for cardiac MR image segmentation trained from a single-scanner dataset to generalize well across multi-scanner and multi-site datasets. Zhang et al. (2019b) applied a similar data augmentation approach to improve the model generalization ability on unseen datasets. Their method has been verified on three tasks including left atrial segmentation from 3D MRI and left ventricle segmentation from 3D ultrasound images. However, effectively designing such a pipeline requires expertise, which may not be easy to be extended to other applications. Most recently, several researchers have begun to investigate the use of generative models (e.g. GANs, variational AE (Kingma and Welling, 2013)), reinforcement learning (Cubuk et al., 2019) and adversarial example generation (Volpi et al., 2018) that aim at directly learning data augmentation strategies from existing data. In particular, the generative model-based approach has been proven to be effective for one-shot brain segmentation (Zhao et al., 2019) and few-shot cardiac MR image segmentation (Chaitanya et al., 2019) and is thus worth to be explored for more applications in the future.

4.3 Lack of Model Interpretability

Unlike symbolic artificial intelligence systems, deep learning systems are difficult to interpret and not transparent. Once a network has been trained, it behaves like a ‘black box’, providing predictions which are not directly interpretable. This issue makes the model unpredictable, intractable for model verification, and ultimately untrustworthy. Recent studies have shown that deep learning-based vision recognition systems can be attacked by images modified with nearly imperceptible

perturbations (Szegedy et al., 2014; Kurakin et al., 2017; Goodfellow et al., 2015). These attacks can also happen in medical scenarios, e.g. a DL-based system may make a wrong diagnosis given an image with adversarial noise or even just small rotation, as demonstrated in a very recent paper (Finlayson et al., 2019). Although there is no denying that deep learning has become a very powerful tool for image analysis, building resilient algorithms robust to potential attacks remains an unsolved problem. One potential solution, instead of building the resilience into the model, is raising failure awareness of the deployed networks. This can be achieved by providing users with segmentation quality scores (Robinson et al., 2019) or confidence maps such as uncertainty maps (Sander et al., 2019) and attention maps (Heo et al., 2018). These scores or maps can be used as evidence to alert users when failure happens. For example, Sander et al. (2019) built a network that is able to simultaneously predict the segmentation mask over cardiac structures and its associated spatial uncertainty map, where the latter one could be used to highlight potential incorrect regions. Such uncertainty information could alert human experts for further justification and refinement in a human-in-the-loop setting.

4.4 Future work

Smart imaging. We have shown that deep learning-based methods are able to segment images in real-time with good accuracy. However, these algorithms can still fail on those image acquisitions with low image quality or significant artifacts. Although there have been several algorithms developed to avoid this problem by either checking the image quality before follow-up studies (Ruijsink et al., 2019; Tarroni et al., 2019), or predicting the segmentation quality to detect failures (Peng and Zhang, 2012; Robinson et al., 2019; Zhou et al., 2019), the development of algorithms that can give instant feedback to correct and optimize the image acquisition process is also important despite less explored. Improving the imaging quality can greatly improve the effectiveness of medical imaging as well as the accuracy of imaging-based diagnosis.

For radiologists, however, finding the optimal imaging and reconstruction parameters to scan each patient can take a great amount of time. Therefore, a DL-based system that has the potential of efficiently and effectively improving the image quality with less noise is of great need. Some researchers have utilized learning-based methods (mostly are deep learning-based) for better image resolution (Oktay et al., 2016), view planning (Alansary et al., 2018), motion correction (Dangi et al., 2018a; Tarroni et al., 2018), artifacts reduction (Oksuz et al., 2019), shadow detection (Meng et al., 2019) and noise reduction (Wolterink et al., 2017b) after image acquisition. However, combining these algorithms with segmentation algorithms and seamlessly integrating them into an efficient, patient-specific imaging system for high-quality image analysis and diagnosis is still an open challenge. An alternative approach is to directly predict cardiac segmentation maps from undersampled k-space data to accelerate the whole procedure, which bypasses the image reconstruction stage (Schlemper et al., 2018).

Data harmonization. A number of works have reported the existence of missing labels and inconsistent labeling protocols among different cardiac image datasets (Zheng et al., 2018; Chen et al., 2019a). Variations have been found in defining the end of basal slices as well as the endocardial wall of myocardium (some include papillary muscles as part of the endocardial contours whereas others do not). These inconsistencies can be a major obstacle for transferring, evaluating and deploying deep learning models trained from one domain (e.g. hospital) to another. Therefore, building a standard benchmark dataset like CheXpert (Irvin et al., 2019) that 1) is *large* enough to have substantial data diversity that reflects the spectrum of real-world diversity; 2) has a *standard* labeling protocol approved by experts, is indeed a need. However, directly building such a dataset from scratch is time-consuming and expensive. A more promising way might be developing an automated tool to combine existing datasets from multiple sources and then to harmonize them to a unified, high-quality dataset.

This tool can not only open the door for crowdsourcing but also enable the rapid deployment of those DL-based segmentation models.

Data privacy. As deep learning is a data-driven approach, an unavoidable and rife concern is about the data privacy. Regulations such as The General Data Protection Regulation (GDPR) now play an important role to protect users' privacy and have forced organizations to treat data ownership seriously. On the other hand, from a technical point of view, how to store, query, and process data such that there is no privacy concerns for building deep learning systems has now become an even more difficult but interesting challenge. Building a privacy-preserving algorithm requires to combine cryptography and deep learning together and to mix techniques from a wide range of subjects such as data analysis, distributed computing, federated learning, differential privacy, in order to achieve models with strong security, fast run time, and great generalizability (Dwork and Roth, 2014; Abadi et al., 2016; Bonawitz et al., 2017; Ryffel et al., 2018). In this respect, Papernot (2018) published a report for guidance, which summarized a set of best practices for improving the privacy and security of machine learning systems. Yet, this field is still in its infancy.

5 CONCLUSION

In this review paper, we provided a comprehensive overview of these deep learning techniques used in three common imaging modalities (MRI, CT, US), covering a wide range of existing deep learning approaches (mostly are CNN-based) that are designed for segmenting different cardiac anatomical structures (e.g. cardiac ventricle, atria, vessel). In particular, we presented and discussed recent progress of deep learning-based segmentation methods in the three modalities, outlined future potential and the remaining limitations of these deep learning-based cardiac segmentation methods that may hinder widespread clinical deployment. We hope that this review can provide an intuitive understanding of those

deep learning-based techniques that have made a significant contribution to cardiac image segmentation and also increase the awareness of common challenges in this field that call for future contribution.

ABBREVIATIONS

Imaging-related terminology: CT: computed tomography; CTA: computed tomography angiography; LAX: long-axis; MPR: multi-planar reformatted; MR: magnetic resonance; MRI: magnetic resonance imaging; LGE: late gadolinium enhancement; RFCA: radio-frequency catheter ablation; SAX: short-axis; US: ultrasound; 2CH: 2-chamber; 3CH: 3-chamber; 4CH: 4-chamber.

Cardiac structures and indexes: AF: atrial fibrillation; AS: aortic stenosis; AO: aorta; CVD: cardiovascular diseases; CAC: coronary artery calcium; DCM: dilated cardiomyopathy; ED: end-diastole; ES: end-systole; EF: ejection fraction; HCM: hypertrophic cardiomyopathy; LA: left atrium; LV: left ventricle; LVEDV: left ventricular end-diastolic volume; LVESV: left ventricular end-systolic volume; MCP: mixed-calcified plaque; MI: myocardial infarction; MYO: myocardium; NCP: non-calcified plaque; PA: pulmonary artery; PV: pulmonary vein; RA: right atrium; RV: right ventricle; RVEDV: right ventricular end-diastolic volume; RVESV: right ventricular end-systolic volume; RVEF: right ventricular ejection fraction; WHS: whole heart segmentation.

Machine learning terminology: AE: autoencoder; ASM: active shape model; BN: batch normalization; CNN: convolutional neural network; CRF: conditional random field; DBN: deep belief network; DL: deep learning; DNN: deep neural network; EM: expectation maximization; FCN: fully convolutional neural network; GAN: generative adversarial network; GRU: gated recurrent units; MSE: mean squared error; MSL: marginal space learning; MRF: markov random field; LSTM: Long-short term memory; ReLU: rectified linear unit; RNN: recurrent neural network; ROI: region-of-interest; SMC: sequential monte carlo; SRF: structured random forest; SVM: support vector

machine.

Cardiac image segmentation datasets: ACDC: Automated Cardiac Diagnosis Challenge; CETUS: Challenge on Endocardial Three-dimensional Ultrasound Segmentation; MM-WHS: Multi-Modality Whole Heart Segmentation; LASC: Left Atrium Segmentation Challenge; LVSC: Left Ventricle Segmentation Challenge; RVSC: Right Ventricle Segmentation Challenge.

Others: EMBC: The International Engineering in Medicine and Biology Conference; GDPR: The General Data Protection Regulation; GPU: graphic processing unit; FDA: United States Food and Drug Administration; ISBI: The IEEE International Symposium on Biomedical Imaging; MICCAI: International Conference on Medical Image Computing and Computer-assisted Intervention; TPU: tensor processing unit; WHO: World Health Organization.

CONFLICT OF INTEREST STATEMENT

The authors declare that the research was conducted in the absence of any commercial or financial relationships that could be construed as a potential conflict of interest.

AUTHOR CONTRIBUTIONS

CC, WB, DR conceived and designed the work; CC, CQ, HQ searched and read the MR, CT, US literature, respectively; CC, CQ, HQ drafted the manuscript together; WB, DR, GT, JD provided critical revision with insightful and constructive comments to improve the manuscript; All authors read and approved the manuscript.

FUNDING

This work is supported by the SmartHeart EPSRC Programme Grant (EP/P001009/1). Huaqi Qiu is supported by the EPSRC Programme Grant (EP/R005982/1).

DATA AVAILABILITY STATEMENT

The datasets summarized in Table 6 can be found in their corresponding websites listed below:

1. York: <http://www.cse.yorku.ca/~mridataset/>
2. Sunnybrook: <http://www.cardiacatlas.org/studies/sunnybrook-cardiac-data/>
3. LVSC: <http://www.cardiacatlas.org/challenges/lv-segmentation-challenge/>
4. RVSC: <http://www.litislabs.fr/?projet=1rvsc>
5. cDEMIRIS: https://www.doc.ic.ac.uk/~rkarim/la_lv_framework/fibrosis
6. LVIC: https://www.doc.ic.ac.uk/~rkarim/la_lv_framework/lv_infarct
7. LASC'13: www.cardiacatlas.org/challenges/left-atrium-segmentation-challenge/
8. HVSMR: <http://segchd.csail.mit.edu/>
9. ACDC: <https://acdc.creatis.insa-lyon.fr/>
10. LASC'18: <http://atriaseg2018.cardiacatlas.org/data/>
11. MM-WHS: <http://www.sdspeople.fudan.edu.cn/zhuangxiahai/0/mmwhs17/>
12. CAT08: <http://coronary.bigr.nl/centerlines/>
13. CLS12: <http://coronary.bigr.nl/stenoses>
14. CETUS: <https://www.creatis.insa-lyon.fr/Challenge/CETUS>
15. CAMUS: <https://www.creatis.insa-lyon.fr/Challenge/camus>

ACKNOWLEDGMENTS

We would like to thank our colleagues: Karl Hahn, Qingjie Meng, James Batten, and Jonathan Passerat-Palmbach who provided insight and expertise that greatly assisted the work, and also constructive and thoughtful comments from Turkey Kart that greatly improved the manuscript.

REFERENCES

- Abadi, M., Chu, A., Goodfellow, I. J., McMahan, H. B., Mironov, I., Talwar, K., et al. (2016). Deep learning with differential privacy. In *the 2016 ACM SIGSAC Conference on Computer and Communications Security, Vienna, Austria, October 24-28, 2016*. 308–318
- Agatston, A. S., Janowitz, W. R., Hildner, F. J., Zusmer, N. R., Viamonte, M., and Detrano, R. (1990). Quantification of coronary artery calcium using ultrafast computed tomography. *Journal of the American College of Cardiology* 15, 827–832
- Alansary, A., Folgoc, L. L., Vaillant, G., Oktay, O., Li, Y., Bai, W., et al. (2018). Automatic view planning with multi-scale deep reinforcement learning agents. In *Medical Image Computing and Computer Assisted Intervention*. 277–285. doi:10.1007/978-3-030-00928-1_32
- Andreopoulos, A. and Tsotsos, J. K. (2008). Efficient and generalizable statistical models of shape and appearance for analysis of cardiac MRI. *Medical image analysis* 12, 335–357. doi:10.1016/j.media.2007.12.003
- Avendi, M. R., Kheradvar, A., and Jafarkhani, H. (2016). A combined deep-learning and deformable-model approach to fully automatic segmentation of the left ventricle in cardiac mri. *Medical Image Analysis* 30, 108–119
- Avendi, M. R., Kheradvar, A., and Jafarkhani, H. (2017). Automatic segmentation of the right ventricle from cardiac MRI using a learning-based approach. *Magnetic resonance in medicine: official journal*

- of the Society of Magnetic Resonance in Medicine / Society of Magnetic Resonance in Medicine 78, 2439–2448. doi:10.1002/mrm.26631
- Bai, W., Chen, C., Tarroni, G., Duan, J., Guitton, F., Petersen, S. E., et al. (2019). Self-Supervised learning for cardiac MR image segmentation by anatomical position prediction. In *Medical Image Computing and Computer Assisted Intervention*. 541–549. doi:10.1007/978-3-030-32245-8_60
- Bai, W., Oktay, O., Sinclair, M., Suzuki, H., Rajchl, M., Tarroni, G., et al. (2017). Semi-supervised learning for Network-Based cardiac MR image segmentation. In *Medical Image Computing and Computer Assisted Intervention*, eds. M. Descoteaux, L. Maier-Hein, A. Franz, P. Jannin, D. L. Collins, and S. Duchesne (Springer International Publishing), vol. 10434, 253–260
- Bai, W., Sinclair, M., Tarroni, G., Oktay, O., Rajchl, M., Vaillant, G., et al. (2018a). Automated cardiovascular magnetic resonance image analysis with fully convolutional networks. *Journal of Cardiovascular Magnetic Resonance* 20, 65
- Bai, W., Suzuki, H., Qin, C., Tarroni, G., Oktay, O., Matthews, P. M., et al. (2018b). Recurrent neural networks for aortic image sequence segmentation with sparse annotations. In *Medical Image Computing and Computer Assisted Intervention*. 586–594. doi:10.1007/978-3-030-00937-3_67
- Baumgartner, C. F., Koch, L. M., Pollefeys, M., and Konukoglu, E. (2017). An exploration of 2D and 3D deep learning techniques for cardiac MR image segmentation. In *International Workshop on Statistical Atlases and Computational Models of the Heart*. 1–8
- Bello, G. A., Dawes, T. J. W., Duan, J., Biffi, C., de Marvao, A., Howard, L. S. G. E., et al. (2019). Deep learning cardiac motion analysis for human survival prediction. *Nature machine intelligence* 1, 95–104. doi:10.1038/s42256-019-0019-2
- Bernard, O., Bosch, J. G., Heyde, B., Alessandrini, M., Barbosa, D., Camarasu-Pop, S., et al. (2016). Standardized evaluation system for left ventricular segmentation algorithms in 3D echocardiography. *IEEE transactions on medical imaging* 35, 967–977. doi:10.1109/TMI.2015.2503890
- Bernard, O., Lalande, A., Zotti, C., Cervenansky, F., Yang, X., Heng, P.-A., et al. (2018). Deep learning techniques for automatic MRI cardiac Multi-Structures segmentation and diagnosis: Is the problem solved? *IEEE Transactions on Medical Imaging* 37, 2514–2525. doi:10.1109/TMI.2018.2837502. <https://acdc.creatis.insa-lyon.fr/>
- Bian, C., Yang, X., Ma, J., Zheng, S., Liu, Y.-A., Nezafat, R., et al. (2018). Pyramid network with online hard example mining for accurate left atrium segmentation. In *Statistical Atlases and Computational Models of the Heart. Atrial Segmentation and LV Quantification Challenges 2018* (Springer International Publishing), 237–245. doi:10.1007/978-3-030-12029-0_26
- Biffi, C., Oktay, O., Tarroni, G., Bai, W., De Marvao, A., Doumou, G., et al. (2018). Learning interpretable anatomical features through deep generative models: Application to cardiac remodeling. In *Medical Image Computing and Computer Assisted Intervention*. vol. 11071 LNCS, 464–471. doi:10.1007/978-3-030-00934-2_52
- Bonawitz, K., Ivanov, V., Kreuter, B., Marcedone, A., McMahan, H. B., Patel, S., et al. (2017). Practical secure aggregation for privacy-preserving machine learning. In *the 2017 ACM SIGSAC Conference on Computer and Communications Security, CCS 2017, Dallas, TX, USA, October 30 - November 03, 2017*. 1175–1191. doi:10.1145/3133956.3133982
- Can, Y. B., Chaitanya, K., Mustafa, B., Koch, L. M., Konukoglu, E., and Baumgartner, C. F. (2018). Learning to segment medical images with Scribble-Supervision alone. In *Deep Learning in Medical Image Analysis and Multimodal Learning for Clinical Decision Support* (Springer International Publishing), 236–244

- Cano-Espinosa, C., González, G., Washko, G. R., Cazorla, M., and Estépar, R. S. J. (2018). Automated Agatston score computation in non-ECG gated CT scans using deep learning. In *Medical Imaging 2018: Image Processing* (International Society for Optics and Photonics), vol. 10574, 105742K
- Carminati, M. C., Boniotti, C., Fusini, L., Andreini, D., Pontone, G., Pepi, M., et al. (2016). Comparison of image processing techniques for nonviable tissue quantification in late gadolinium enhancement cardiac magnetic resonance images. *Journal of thoracic imaging* 31, 168–176. doi:10.1097/RTI.0000000000000206
- Carneiro, G., Nascimento, J., and Freitas, A. (2010). Robust left ventricle segmentation from ultrasound data using deep neural networks and efficient search methods. In *2010 IEEE International Symposium on Biomedical Imaging: From Nano to Macro*. 1085–1088
- Carneiro, G. and Nascimento, J. C. (2010). Multiple dynamic models for tracking the left ventricle of the heart from ultrasound data using particle filters and deep learning architectures. In *Conference on Computer Vision and Pattern Recognition (IEEE)*, 2815–2822
- Carneiro, G. and Nascimento, J. C. (2011). Incremental on-line semi-supervised learning for segmenting the left ventricle of the heart from ultrasound data. In *2011 International Conference on Computer Vision (IEEE)*, 1700–1707
- Carneiro, G. and Nascimento, J. C. (2012). The use of on-line co-training to reduce the training set size in pattern recognition methods: Application to left ventricle segmentation in ultrasound. In *Conference on Computer Vision and Pattern Recognition (IEEE)*, 948–955
- Carneiro, G. and Nascimento, J. C. (2013). Combining multiple dynamic models and deep learning architectures for tracking the left ventricle endocardium in ultrasound data. *IEEE transactions on pattern analysis and machine intelligence* 35, 2592–2607
- Carneiro, G., Nascimento, J. C., and Freitas, A. (2012). The segmentation of the left ventricle of the heart from ultrasound data using deep learning architectures and derivative-based search methods. *IEEE Transactions on Image Processing* 21, 968–982. doi:10.1109/TIP.2011.2169273
- Castro, F. M., Marín-Jiménez, M. J., Guil, N., Schmid, C., and Alahari, K. (2018). End-to-end incremental learning. In *European Conference on Computer Vision*. 241–257. doi:10.1007/978-3-030-01258-8\15
- Chaitanya, K., Karani, N., Baumgartner, C., Donati, O., Becker, A., and Konukoglu, E. (2019). Semi-Supervised and Task-Driven data augmentation. In *International Conference on Information Processing in Medical Imaging*. 29–41. doi:10.1007/978-3-030-20351-1\3
- Chartsias, A., Joyce, T., Papanastasiou, G., Semple, S., Williams, M., Newby, D., et al. (2018). Factorised spatial representation learning: Application in semi-supervised myocardial segmentation. In *Medical Image Computing and Computer Assisted Intervention*. vol. 11071 LNCS, 490–498
- Chen, C., Bai, W., Davies, R. H., Bhuva, A. N., Manisty, C., Moon, J. C., et al. (2019a). Improving the generalizability of convolutional neural network-based segmentation on CMR images. *Arxiv Preprint abs/1907.01268*. Available at <http://arxiv.org/abs/1907.01268> (Accessed September 1, 2019)
- Chen, C., Bai, W., and Rueckert, D. (2018a). Multi-task learning for left atrial segmentation on GE-MRI. In *9th International Workshop, STACOM 2018, Held in Conjunction with MICCAI 2018, Granada, Spain, September 16, 2018*, (Springer International Publishing), 292–301. doi:10.1007/978-3-030-12029-0\32
- Chen, C., Biffi, C., Tarroni, G., Petersen, S., Bai, W., and Rueckert, D. (2019b). Learning shape priors for robust cardiac MR segmentation from multi-view images. In *Medical Image Computing and Computer Assisted Intervention*. 523–531

- Chen, C., Dou, Q., Zhou, J., Qin, J., and Heng, P. A. (2019c). Synergistic image and feature adaptation: Towards Cross-Modality domain adaptation for medical image segmentation. *Conference on Artificial Intelligence*, 865–872. doi:10.1609/aaai.v33i01.3301865
- Chen, H., Zheng, Y., Park, J.-H., Heng, P.-A., and Zhou, S. K. (2016). Iterative multi-domain regularized deep learning for anatomical structure detection and segmentation from ultrasound images. In *Medical Image Computing and Computer-Assisted Intervention – MICCAI 2016* (Springer International Publishing), 487–495
- Chen, J., Yang, G., Gao, Z., Ni, H., Firmin, D., and others (2018b). Multiview two-task recursive attention model for left atrium and atrial scars segmentation. In *Medical Image Computing and Computer Assisted Intervention*. 455–463. doi:10.1007/978-3-030-00934-2_51
- Chen, J., Zhang, H., Zhang, Y., Zhao, S., Mohiaddin, R., Wong, T., et al. (2019d). Discriminative consistent domain generation for semi-supervised learning. In *Medical Image Computing and Computer Assisted Intervention*. 595–604. doi:10.1007/978-3-030-32245-8_66
- Chen, L.-C., Papandreou, G., Schroff, F., and Adam, H. (2017). Rethinking atrous convolution for semantic image segmentation. *Arxiv Preprint* abs/1706.05587. Available at <http://arxiv.org/abs/1706.05587> (Accessed September 1, 2019)
- Chen, M., Fang, L., and Liu, H. (2019e). FR-NET: Focal loss constrained deep residual networks for segmentation of cardiac MRI. In *International Symposium on Biomedical Imaging*. 764–767. doi:10.1109/ISBI.2019.8759556
- Chen, S., Ma, K., and Zheng, Y. (2019f). Med3d: Transfer learning for 3d medical image analysis. *Arxiv Preprint* abs/1904.00625. Available at <http://arxiv.org/abs/1904.00625> (Accessed September 1, 2019)
- Chen, X., Williams, B. M., Vallabhaneni, S. R., Czanner, G., Williams, R., and Zheng, Y. (2019g). Learning active contour models for medical image segmentation. In *Conference on Computer Vision and Pattern Recognition*. 11632–11640
- Chen, Y.-C., Lin, Y.-C., Wang, C.-P., Lee, C.-Y., Lee, W.-J., Wang, T.-D., et al. (2019h). Coronary artery segmentation in cardiac CT angiography using 3D multi-channel U-net. In *Medical Imaging with Deep Learning*. 1907.12246
- Cho, K., van Merriënboer, B., Gulcehre, C., Bahdanau, D., Bougares, F., Schwenk, H., et al. (2014). Learning phrase representations using RNN Encoder-Decoder for statistical machine translation. In *Conference on Empirical Methods in Natural Language Processing (ACL)*, 1724–1734
- Çiçek, Ö., Abdulkadir, A., Lienkamp, S. S., Brox, T., and Ronneberger, O. (2016). 3D U-Net: Learning dense volumetric segmentation from sparse annotation. In *Medical Image Computing and Computer Assisted Intervention*. 424–432. doi:10.1007/978-3-319-46723-8_49
- Ciresan, D. C. and Giusti, A. (2012). Deep neural networks segment neuronal membranes in electron microscopy images. In *Conference on Neural Information Processing Systems*. 2852–2860
- Clough, J. R., Oksuz, I., Byrne, N., Schnabel, J. A., and King, A. P. (2019). Explicit topological priors for deep-learning based image segmentation using persistent homology. In *Information Processing in Medical Imaging*. vol. 11492 LNCS, 16–28. doi:10.1007/978-3-030-20351-1_2
- Cong, C. and Zhang, H. (2018). Invert-U-Net DNN segmentation model for MRI cardiac left ventricle segmentation. *The Journal of Engineering* 2018, 1463–1467. doi:10.1049/joe.2018.8302
- Cubuk, E. D., Zoph, B., Mane, D., Vasudevan, V., and Le, Q. V. (2019). Autoaugment: Learning augmentation policies from data. In *Conference on Computer Vision and Pattern Recognition*. 1–14

- Dangi, S., Linte, C. A., and Yaniv, Z. (2018a). Cine cardiac MRI slice misalignment correction towards full 3D left ventricle segmentation. In *Proceedings of SPIE The International Society for Optical Engineering*. 1057607. doi:10.1117/12.2294936
- Dangi, S., Yaniv, Z., and Linte, C. A. (2018b). Left ventricle segmentation and quantification from cardiac cine MR images via multi-task learning. In *Statistical Atlases and Computational Models of the Heart. Atrial Segmentation and LV Quantification Challenges - 9th International Workshop, STACOM 2018, Held in Conjunction with MICCAI 2018, Granada, Spain, September 16, 2018, Revised Selected Papers*. 21–31. doi:10.1007/978-3-030-12029-0_3
- de Vos, B. D., Wolterink, J. M., De Jong, P. A., Leiner, T., Viergever, M. A., and Isgum, I. (2017). Convnet-based localization of anatomical structures in 3-D medical images. *IEEE Transactions on Medical Imaging* 36, 1470–1481
- de Vos, B. D., Wolterink, J. M., Leiner, T., de Jong, P. A., Lessmann, N., and Isgum, I. (2019). Direct automatic coronary calcium scoring in cardiac and chest CT. *IEEE Transactions on Medical Imaging* 38, 2127–2138
- Degel, M. A., Navab, N., and Albarqouni, S. (2018). Domain and geometry agnostic CNNs for left atrium segmentation in 3D ultrasound. In *Medical Image Computing and Computer Assisted Intervention – MICCAI 2018* (Springer International Publishing), 630–637
- Dong, S., Luo, G., Wang, K., Cao, S., Li, Q., and Zhang, H. (2018a). A combined fully convolutional networks and deformable model for automatic left ventricle segmentation based on 3D echocardiography. *Biomed Res. Int.* 2018, 5682365. doi:10.1155/2018/5682365
- Dong, S., Luo, G., Wang, K., Cao, S., Mercado, A., Shmuilovich, O., et al. (2018b). VoxelAtlasGAN: 3D left ventricle segmentation on echocardiography with atlas guided generation and Voxel-to-Voxel discrimination. In *Medical Image Computing and Computer Assisted Intervention – MICCAI 2018* (Springer International Publishing), 622–629
- Dormer, J. D., Ma, L., Halicek, M., Reilly, C. M., Schreiber, E., and Fei, B. (2018). Heart chamber segmentation from CT using convolutional neural networks. In *Medical Imaging 2018: Biomedical Applications in Molecular, Structural, and Functional Imaging, Houston, Texas, United States, 10-15 February 2018*. 105782S
- Dou, Q., Ouyang, C., Chen, C., Chen, H., Glocker, B., Zhuang, X., et al. (2019). Pnp-adanet: Plug-and-play adversarial domain adaptation network at unpaired cross-modality cardiac segmentation. *IEEE Access* 7, 99065–99076. doi:10.1109/ACCESS.2019.2929258
- Dou, Q., Ouyang, C., Chen, C., Chen, H., and Heng, P.-A. (2018). Unsupervised Cross-Modality domain adaptation of ConvNets for biomedical image segmentations with adversarial loss. In *International Joint Conferences on Artificial Intelligence*. 691–697
- Du, X., Yin, S., Tang, R., Zhang, Y., and Li, S. (2019). Cardiac-DeepIED: Automatic pixel-level deep segmentation for cardiac bi-ventricle using improved end-to-end encoder-decoder network. *IEEE journal of translational engineering in health and medicine* 7, 1–10. doi:10.1109/JTEHM.2019.2900628
- Duan, J., Bello, G., Schlemper, J., Bai, W., Dawes, T. J. W., Biffi, C., et al. (2019). Automatic 3D bi-ventricular segmentation of cardiac images by a shape-constrained multi-task deep learning approach. *IEEE Transactions on Medical Imaging* PP, 1. doi:10.1109/TMI.2019.2894322
- Duan, J., Schlemper, J., Bai, W., Dawes, T. J. W., Bello, G., Doumou, G., et al. (2018a). Deep nested level sets: Fully automated segmentation of cardiac MR images in patients with pulmonary hypertension. In *Medical Image Computing and Computer Assisted Intervention*. 595–603

- Duan, Y., Feng, J., Lu, J., and Zhou, J. (2018b). Context aware 3D fully convolutional networks for coronary artery segmentation. In *International Workshop on Statistical Atlases and Computational Models of the Heart* (Springer), 85–93
- Dwork, C. and Roth, A. (2014). The algorithmic foundations of differential privacy. *Foundations and Trends in Theoretical Computer Science* 9, 211–407
- Fahmy, A. S., El-Rewaidy, H., Nezafat, M., Nakamori, S., and Nezafat, R. (2019). Automated analysis of cardiovascular magnetic resonance myocardial native T1 mapping images using fully convolutional neural networks. *Journal of Cardiovascular Magnetic Resonance* 21, 1–12. doi:10.1186/s12968-018-0516-1
- Fahmy, A. S., Rausch, J., Neisius, U., Chan, R. H., Maron, M. S., Appelbaum, E., et al. (2018). Automated cardiac MR scar quantification in hypertrophic cardiomyopathy using deep convolutional neural networks. *JACC. Cardiovascular imaging* 11, 1917–1918. doi:10.1016/j.jcmg.2018.04.030
- Finlayson, S. G., Bowers, J. D., Ito, J., Zittrain, J. L., Beam, A. L., and Kohane, I. S. (2019). Adversarial attacks on medical machine learning. *Science* 363, 1287–1289. doi:10.1126/science.aaw4399
- Gandhi, S., Mosleh, W., Shen, J., and Chow, C.-M. (2018). Automation, machine learning, and artificial intelligence in echocardiography: A brave new world. *Echocardiography* 35, 1402–1418. doi:10.1111/echo.14086
- Georgescu, B., Zhou, X. S., Comaniciu, D., and Gupta, A. (2005). Database-guided segmentation of anatomical structures with complex appearance. In *2005 IEEE Computer Society Conference on Computer Vision and Pattern Recognition (CVPR'05)* (IEEE), vol. 2, 429–436
- Ghesu, F. C., Krubasik, E., Georgescu, B., Singh, V., Yefeng Zheng, Hornegger, J., et al. (2016). Marginal space deep learning: Efficient architecture for volumetric image parsing. *IEEE Transactions on Medical Imaging* 35, 1217–1228
- Girdhar, R., Fouhey, D. F., Rodriguez, M., and Gupta, A. (2016). Learning a predictable and generative vector representation for objects. In *European Conference on Computer Vision* (Springer International Publishing), 484–499
- Goodfellow, I. (2016). *Deep learning*. Adaptive computation and machine learning (Cambridge, Massachusetts ; London, England: The MIT Press)
- Goodfellow, I. J., Pouget-Abadie, J., Mirza, M., Xu, B., Warde-Farley, D., Ozair, S., et al. (2014). Generative adversarial networks. In *Conference on Neural Information Processing Systems* (Curran Associates, Inc.), 2672–2680
- Goodfellow, I. J., Shlens, J., and Szegedy, C. (2015). Explaining and harnessing adversarial examples. In *International Conference on Learning Representations*. 43405
- Greenspan, H., Van Ginneken, B., and Summers, R. M. (2016). Guest editorial deep learning in medical imaging: Overview and future promise of an exciting new technique. *IEEE Transactions on Medical Imaging* 35, 1153–1159
- Gülsün, M. A., Funke-Lea, G., Sharma, P., Rapaka, S., and Zheng, Y. (2016). Coronary centerline extraction via optimal flow paths and CNN path pruning. In *Medical Image Computing and Computer Assisted Intervention* (Springer), 317–325
- Guo, Z., Bai, J., Lu, Y., Wang, X., Cao, K., Song, Q., et al. (2019). Deepcenterline: A multi-task fully convolutional network for centerline extraction. In *International Conference on Information Processing in Medical Imaging* (Springer), 441–453
- He, K., Zhang, X., Ren, S., and Sun, J. (2015). Delving deep into rectifiers: Surpassing Human-Level performance on ImageNet classification. In *International Conference on Computer Vision* (IEEE Computer Society), 1026–1034

- He, K., Zhang, X., Ren, S., and Sun, J. (2016). Deep residual learning for image recognition. In *Conference on Computer Vision and Pattern Recognition*. 770–778
- Heo, J., Lee, H. B., Kim, S., Lee, J., Kim, K. J., Yang, E., et al. (2018). Uncertainty-Aware attention for reliable interpretation and prediction. In *Advances in Neural Information Processing Systems 31*, eds. S. Bengio, H. Wallach, H. Larochelle, K. Grauman, N. Cesa-Bianchi, and R. Garnett (Curran Associates, Inc.). 909–918
- Herment, A., Kachenoura, N., Lefort, M., Bensalah, M., Dogui, A., Frouin, F., et al. (2010). Automated segmentation of the aorta from phase contrast MR images: validation against expert tracing in healthy volunteers and in patients with a dilated aorta. *Journal of magnetic resonance imaging* 31, 881–888. doi:10.1002/jmri.22124
- Hinton, G. E. and Salakhutdinov, R. R. (2006). Reducing the dimensionality of data with neural networks. *Science* 313, 504–507
- Hochreiter, S. and Schmidhuber, J. (1997). Long short-term memory. *Neural computation* 9, 1735–1780. doi:10.1162/neco.1997.9.8.1735
- Hu, J., Shen, L., and Sun, G. (2018). Squeeze-and-Excitation networks. In *Conference on Computer Vision and Pattern Recognition*. 7132–7141. doi:10.1109/CVPR.2018.00745
- Huang, G., Liu, Z., van der Maaten, L., and Weinberger, K. Q. (2017). Densely connected convolutional networks. In *Conference on Computer Vision and Pattern Recognition*. 2261–2269
- Huang, Q., Yang, D., Yi, J., Axel, L., and Metaxas, D. (2019). FR-Net: Joint reconstruction and segmentation in compressed sensing cardiac MRI. In *Functional Imaging and Modelling of the Heart* (Springer International Publishing), 352–360. doi:10.1007/978-3-030-21949-9_38
- Huang, W., Huang, L., Lin, Z., Huang, S., Chi, Y., Zhou, J., et al. (2018). Coronary artery segmentation by deep learning neural networks on computed tomographic coronary angiographic images. In *2018 40th Annual International Conference of the IEEE Engineering in Medicine and Biology Society (EMBC)* (IEEE), 608–611
- Ioffe, S. and Szegedy, C. (2015). Batch normalization: accelerating deep network training by reducing internal covariate shift. In *ICML (JMLR.org)*, 448–456
- Irvin, J., Rajpurkar, P., Ko, M., Yu, Y., Ciurea-Ilcus, S., Chute, C., et al. (2019). CheXpert: A large chest radiograph dataset with uncertainty labels and expert comparison. In *Conference on Artificial Intelligence*. 590–597
- Isensee, F., Jaeger, P. F., Full, P. M., Wolf, I., Engelhardt, S., and Maier-Hein, K. H. (2017). Automatic cardiac disease assessment on cine-MRI via Time-Series segmentation and domain specific features. In *Statistical Atlases and Computational Models of the Heart. ACDC and MMWHS Challenges* (Springer International Publishing), 120–129. doi:10.1007/978-3-319-75541-0_13
- Jafari, M. H., Girgis, H., Abdi, A. H., Liao, Z., Pesteie, M., Rohling, R., et al. (2019). Semi-Supervised learning for cardiac left ventricle segmentation using conditional deep generative models as prior. In *2019 IEEE 16th International Symposium on Biomedical Imaging (ISBI 2019)* (IEEE), 649–652
- Jafari, M. H., Girgis, H., Liao, Z., Behnami, D., Abdi, A., Vaseli, H., et al. (2018). A unified framework integrating recurrent Fully-Convolutional networks and optical flow for segmentation of the left ventricle in echocardiography data. In *Deep Learning in Medical Image Analysis and Multimodal Learning for Clinical Decision Support* (Springer International Publishing), 29–37
- Jang, Y., Hong, Y., Ha, S., Kim, S., and Chang, H.-J. (2017). Automatic segmentation of LV and RV in cardiac MRI. In *International Workshop on Statistical Atlases and Computational Models of the Heart* (Springer), 161–169

- Jia, S., Despinasse, A., Wang, Z., Delingette, H., Pennec, X., Jaïs, P., et al. (2018). Automatically segmenting the left atrium from cardiac images using successive 3D U-Nets and a contour loss. In *International Workshop on Statistical Atlases and Computational Models of the Heart*. 221–229
- Joyce, T., Chartsias, A., and Tsaftaris, S. A. (2018). Deep Multi-Class segmentation without Ground-Truth labels. In *Medical Imaging with Deep Learning*. 1–9
- Kamnitsas, K., Bai, W., Ferrante, E., McDonagh, S., and Sinclair, M. (2017a). Ensembles of multiple models and architectures for robust brain tumour segmentation. In *Brainlesion: Glioma, Multiple Sclerosis, Stroke and Traumatic Brain Injuries - Third International Workshop, BrainLes 2017, Held in Conjunction with MICCAI 2017, Quebec City, QC, Canada, September 14, 2017, Revised Selected Papers*. 450–462
- Kamnitsas, K., Baumgartner, C., Ledig, C., Newcombe, V., Simpson, J., Kane, A., et al. (2017b). Unsupervised domain adaptation in brain lesion segmentation with adversarial networks. In *International Conference on Information Processing in Medical Imaging* (Springer International Publishing), 597–609
- Kang, D., Woo, J., Kuo, C. J., Slomka, P. J., Dey, D., and Germano, G. (2012). Heart chambers and whole heart segmentation techniques. *Journal of Electronic Imaging* 21, 010901
- Karim, R., Bhagirath, P., Claus, P., James Housden, R., Chen, Z., Karimaghloo, Z., et al. (2016). Evaluation of state-of-the-art segmentation algorithms for left ventricle infarct from late gadolinium enhancement MR images. *Medical image analysis* 30, 95–107. doi:10.1016/j.media.2016.01.004
- Karim, R., Blake, L.-E., Inoue, J., Tao, Q., Jia, S., James Housden, R., et al. (2018). Algorithms for left atrial wall segmentation and thickness – evaluation on an open-source CT and MRI image database. *Medical Image Analysis* 50, 36–53. doi:10.1016/j.media.2018.08.004
- Karim, R., Housden, R. J., Balasubramaniam, M., Chen, Z., Perry, D., Uddin, A., et al. (2013). Evaluation of current algorithms for segmentation of scar tissue from late gadolinium enhancement cardiovascular magnetic resonance of the left atrium: an open-access grand challenge. *Journal of cardiovascular magnetic resonance: official journal of the Society for Cardiovascular Magnetic Resonance* 15, 105. doi:10.1186/1532-429X-15-105
- Karim, R., Mohiaddin, R., and Rueckert, D. (2008). Left atrium segmentation for atrial fibrillation ablation. In *Medical Imaging 2008: Visualization, Image-Guided Procedures, and Modeling, San Diego, California, United States, 16-21 February 2008* (SPIE), March 2008, 69182U. doi:10.1117/12.771023
- Kass, M., Witkin, A., and Terzopoulos, D. (1988). Snakes: Active contour models. *Int. J. Comput. Vis.* 1, 321–331
- Kervadec, H., Dolz, J., Tang, M., Granger, E., Boykov, Y., and Ben Ayed, I. (2019). Constrained-CNN losses for weakly supervised segmentation. In *Medical Image Analysis*. vol. 54, 88–99. doi:10.1016/j.media.2019.02.009
- Khened, M., Kollerathu, V. A., and Krishnamurthi, G. (2019). Fully convolutional multi-scale residual DenseNets for cardiac segmentation and automated cardiac diagnosis using ensemble of classifiers. *Medical Image Analysis* 51, 21–45. doi:10.1016/j.media.2018.10.004
- Kim, R. J., Fieno, D. S., Parrish, T. B., Harris, K., Chen, E. L., Simonetti, O., et al. (1999). Relationship of MRI delayed contrast enhancement to irreversible injury, infarct age, and contractile function. *Circulation* 100, 1992–2002. doi:10.1161/01.cir.100.19.1992
- Kingma, D. P. and Welling, M. (2013). Auto-Encoding variational bayes. In *International Conference on Learning Representations*. 1–14
- Kirişli, H. A., Schaap, M., Metz, C. T., Dharampal, A. S., Meijboom, W. B., Papadopoulou, S. L., et al. (2013). Standardized evaluation framework for evaluating coronary artery stenosis detection, stenosis quantification and lumen segmentation algorithms in computed tomography angiography. *Medical*

- Image Analysis* 17, 859–876. doi:10.1016/j.media.2013.05.007. <http://coronary.bigr.nl/stenoses>
- Kurakin, A., Goodfellow, I., and Bengio, S. (2017). Adversarial examples in the physical world. In *5th International Conference on Learning Representations, ICLR 2017, Toulon, France, April 24-26, 2017, Workshop Track Proceedings*. 1–14
- Leclerc, S., Smistad, E., Grenier, T., Lartizien, C., Ostvik, A., Espinosa, F., et al. (2018). Deep learning applied to Multi-Structure segmentation in 2D echocardiography: A preliminary investigation of the required database size. In *2018 IEEE International Ultrasonics Symposium (IUS)* (IEEE), 1–4
- Leclerc, S., Smistad, E., Pedrosa, J., Ostvik, A., Cervenansky, F., Espinosa, F., et al. (2019). Deep learning for segmentation using an open Large-Scale dataset in 2D echocardiography. *IEEE Trans. Med. Imaging* <https://www.creatis.insa-lyon.fr/Challenge/camus>
- Lee, C.-Y., Xie, S., Gallagher, P., Zhang, Z., and Tu, Z. (2015). Deeply-Supervised nets. In *Artificial Intelligence and Statistics*. 562–570
- Lee, M. C. H., Petersen, K., Pawlowski, N., Glocker, B., and Schaap, M. (2019). TETRIS: Template transformer networks for image segmentation with shape priors. *IEEE transactions on medical imaging*
- Lesage, D., Angelini, E. D., Bloch, I., and Funka-Lea, G. (2009). A review of 3D vessel lumen segmentation techniques: Models, features and extraction schemes. *Medical Image Analysis* 13, 819–845
- Lessmann, N., Išgum, I., Setio, A. A., de Vos, B. D., Ciompi, F., de Jong, P. A., et al. (2016). Deep convolutional neural networks for automatic coronary calcium scoring in a screening study with low-dose chest CT. In *Medical Imaging 2016: Computer-Aided Diagnosis* (International Society for Optics and Photonics), vol. 9785, 978511
- Lessmann, N., van Ginneken, B., Zreik, M., de Jong, P. A., de Vos, B. D., Viergever, M. A., et al. (2017). Automatic calcium scoring in low-dose chest CT using deep neural networks with dilated convolutions. *IEEE Transactions on Medical Imaging* 37, 615–625
- Li, C., Tong, Q., Liao, X., Si, W., Chen, S., Wang, Q., et al. (2019a). APCP-NET: Aggregated parallel Cross-Scale pyramid network for CMR segmentation. In *2019 IEEE 16th International Symposium on Biomedical Imaging (ISBI 2019)*. 784–788. doi:10.1109/ISBI.2019.8759147
- Li, C., Tong, Q., Liao, X., Si, W., Sun, Y., Wang, Q., et al. (2018). Attention based hierarchical aggregation network for 3D left atrial segmentation: 9th international workshop, STACOM 2018, held in conjunction with MICCAI 2018, granada, spain, september 16, 2018, revised selected papers. In *Statistical Atlases and Computational Models of the Heart. Atrial Segmentation and LV Quantification Challenges*, eds. M. Pop, M. Sermesant, J. Zhao, S. Li, K. McLeod, A. Young, K. Rhode, and T. Mansi (Cham: Springer International Publishing), vol. 11395 of *Lecture Notes in Computer Science*. 255–264. doi:10.1007/978-3-030-12029-0_28
- Li, J., Yu, Z., Gu, Z., Liu, H., and Li, Y. (2019b). Dilated-Inception net: Multi-Scale feature aggregation for cardiac right ventricle segmentation. *IEEE transactions on bio-medical engineering* , 1–1doi:10.1109/TBME.2019.2906667
- Li, J., Zhang, R., Shi, L., and Wang, D. (2017). Automatic Whole-Heart segmentation in congenital heart disease using Deeply-Supervised 3D FCN. In *Reconstruction, Segmentation, and Analysis of Medical Images* (Springer International Publishing), 111–118. doi:10.1007/978-3-319-52280-7_11
- Liao, F., Chen, X., Hu, X., and Song, S. (2019). Estimation of the volume of the left ventricle from MRI images using deep neural networks. *IEEE transactions on cybernetics* 49, 495–504. doi:10.1109/TCYB.2017.2778799
- Lieman-Sifry, J., Le, M., Lau, F., Sall, S., and Golden, D. (2017). FastVentricle: Cardiac segmentation with ENet. In *Functional Imaging and Modelling of the Heart*, eds. M. Pop and G. A. Wright (Cham:

- Springer International Publishing), vol. 10263 LNCS of *Lecture Notes in Computer Science*, 127–138. doi:10.1007/978-3-319-59448-4_13
- Litjens, G., Kooi, T., Bejnordi, B. E., Setio, A. A. A., Ciompi, F., Ghafoorian, M., et al. (2017). A survey on deep learning in medical image analysis. *Medical Image Analysis* 42, 60 – 88
- Liu, J., Jin, C., Feng, J., Du, Y., Lu, J., and Zhou, J. (2018). A vessel-focused 3D convolutional network for automatic segmentation and classification of coronary artery plaques in cardiac CTA. In *International Workshop on Statistical Atlases and Computational Models of the Heart* (Springer), 131–141
- Long, J., Shelhamer, E., and Darrell, T. (2015). Fully convolutional networks for semantic segmentation. In *Conference on Computer Vision and Pattern Recognition*. 3431–3440
- Lu, X., Chen, X., Li, W., and Qiao, Y. (2019). Graph cut segmentation of the right ventricle in cardiac MRI using multi-scale feature learning. In *Proceedings of the 3rd International Conference on Cryptography, Security and Privacy* (ACM), 231–235. doi:10.1145/3309074.3309117
- Luc, P., Couprie, C., Chintala, S., and Verbeek, J. (2016). Semantic segmentation using adversarial networks. In *NIPS Workshop on Adversarial Training*. 1–12
- Ma, J. and Zhang, R. (2019). Automatic calcium scoring in cardiac and chest CT using DenseRAUnet. *Arxiv Preprint* abs/1907.11392. Available at <http://arxiv.org/abs/1907.11392> (Accessed September 1, 2019)
- Mahapatra, D., Bozorgtabar, B., Thiran, J.-P., and Reyes, M. (2018). Efficient active learning for image classification and segmentation using a sample selection and conditional generative adversarial network. In *Medical Image Computing and Computer Assisted Intervention* (Springer International Publishing), 580–588. doi:10.1007/978-3-030-00934-2_65
- Mazurowski, M. A., Buda, M., Saha, A., and Bashir, M. R. (2019). Deep learning in radiology: An overview of the concepts and a survey of the state of the art with focus on MRI. *Journal of magnetic resonance imaging* 49, 939–954. doi:10.1002/jmri.26534
- Medley, D. O., Santiago, C., and Nascimento, J. C. (2019). Segmenting the left ventricle in cardiac in cardiac MRI: From handcrafted to deep region based descriptors. In *2019 IEEE 16th International Symposium on Biomedical Imaging (ISBI 2019)*. 644–648. doi:10.1109/ISBI.2019.8759179
- Meng, Q., Sinclair, M., Zimmer, V., Hou, B., Rajchl, M., Toussaint, N., et al. (2019). Weakly supervised estimation of shadow confidence maps in fetal ultrasound imaging. *IEEE Transactions on Medical Imaging*
- Merkow, J., Marsden, A., Kriegman, D., and Tu, Z. (2016). Dense volume-to-volume vascular boundary detection. In *Medical Image Computing and Computer Assisted Intervention* (Springer), 371–379
- Milletari, F., Navab, N., and Ahmadi, S. (2016). V-Net: Fully convolutional neural networks for volumetric medical image segmentation. In *2016 Fourth International Conference on 3D Vision (3DV)*. 565–571. doi:10.1109/3DV.2016.79
- Moccia, S., Banali, R., Martini, C., Muscogiuri, G., Pontone, G., Pepi, M., et al. (2019). Development and testing of a deep learning-based strategy for scar segmentation on CMR-LGE images. *Magnetic Resonance Materials in Physics, Biology and Medicine* 32, 187–195. doi:10.1007/s10334-018-0718-4
- Moeskops, P., Wolterink, J. M., van der Velden, B. H., Gilhuijs, K. G., Leiner, T., Viergever, M. A., et al. (2016). Deep learning for multi-task medical image segmentation in multiple modalities. In *Medical Image Computing and Computer Assisted Intervention* (Springer), 478–486
- Mortazi, A., Burt, J., and Bagci, U. (2017a). Multi-planar deep segmentation networks for cardiac substructures from MRI and CT. In *International Workshop on Statistical Atlases and Computational Models of the Heart* (Springer), 199–206

- Mortazi, A., Karim, R., Rhode, K., Burt, J., and Bagci, U. (2017b). CardiacNET: Segmentation of left atrium and proximal pulmonary veins from MRI using multi-view CNN. In *Lecture Notes in Computer Science (including subseries Lecture Notes in Artificial Intelligence and Lecture Notes in Bioinformatics)*. 377–385. doi:10.1007/978-3-319-66185-8_43
- Nascimento, J. C. and Carneiro, G. (2014). Non-rigid segmentation using sparse low dimensional manifolds and deep belief networks. In *Proceedings of the IEEE Conference on Computer Vision and Pattern Recognition (cv-foundation.org)*, 288–295
- Nascimento, J. C. and Carneiro, G. (2017). Deep learning on sparse manifolds for faster object segmentation. *IEEE Transactions on Image Processing* 26, 4978–4990
- Nascimento, J. C. and Carneiro, G. (2019). One shot segmentation: unifying rigid detection and non-rigid segmentation using elastic regularization. *IEEE Trans. Pattern Anal. Mach. Intell.* doi:10.1109/TPAMI.2019.2922959
- Ngo, T. A., Lu, Z., and Carneiro, G. (2017). Combining deep learning and level set for the automated segmentation of the left ventricle of the heart from cardiac cine magnetic resonance. *Medical Image Analysis* 35, 159–171
- Noble, J. A. and Boukerroui, D. (2006). Ultrasound image segmentation: a survey. *IEEE Transactions on Medical Imaging* 25, 987–1010. doi:10.1109/TMI.2006.877092
- Oksuz, I., Clough, J., Bai, W., Ruijsink, B., Puyol-Antón, E., Cruz, G., et al. (2019). High-quality segmentation of low quality cardiac MR images using k-space artefact correction. In *Medical Imaging with Deep Learning*, eds. M. J. Cardoso, A. Feragen, B. Glocker, E. Konukoglu, I. Oguz, G. Unal, and T. Vercauteren (London, United Kingdom: PMLR), vol. 102 of *Proceedings of Machine Learning Research*, 380–389
- Oktay, O., Bai, W., Lee, M., Guerrero, R., Kamnitsas, K., Caballero, J., et al. (2016). Multi-input cardiac image super-resolution using convolutional neural networks. In *Medical Image Computing and Computer Assisted Intervention*. vol. 9902 LNCS, 246–254. doi:10.1007/978-3-319-46726-9_29
- Oktay, O., Ferrante, E., Kamnitsas, K., Heinrich, M., Bai, W., Caballero, J., et al. (2018a). Anatomically constrained neural networks (acnns): Application to cardiac image enhancement and segmentation. *IEEE Transactions on Medical Imaging* 37, 384–395
- Oktay, O., Schlemper, J., Folgoc, L. L., Lee, M., Heinrich, M., Misawa, K., et al. (2018b). Attention U-Net: Learning where to look for the pancreas. In *Medical Imaging with Deep Learning*. 1804.03999
- Ouyang, C., Kamnitsas, K., Biffi, C., Duan, J., and Rueckert, D. (2019). Data efficient unsupervised domain adaptation for Cross-Modality image segmentation. In *Medical Image Computing and Computer Assisted Intervention*. 669–677
- Pace, D. F., Dalca, A. V., Geva, T., Powell, A. J., Moghari, M. H., and Golland, P. (2015). Interactive Whole-Heart segmentation in congenital heart disease. *Medical image computing and computer-assisted intervention: MICCAI ... International Conference on Medical Image Computing and Computer-Assisted Intervention* 9351, 80–88. doi:10.1007/978-3-319-24574-4_10. <http://segchd.csail.mit.edu/>
- Painchaud, N., Skandarani, Y., Judge, T., Bernard, O., Lalande, A., and Jodoin, P.-M. (2019). Cardiac MRI segmentation with strong anatomical guarantees. In *Medical Image Computing and Computer Assisted Intervention*. 632–640
- Papernot, N. (2018). A marauder’s map of security and privacy in machine learning: An overview of current and future research directions for making machine learning secure and private. In *the 11th ACM Workshop on Artificial Intelligence and Security, CCS 2018, Toronto, ON, Canada, October 19, 2018*. 1. doi:10.1145/3270101.3270102

- Patravali, J., Jain, S., and Chilamkurthy, S. (2017). 2d-3d fully convolutional neural networks for cardiac mr segmentation. In *Statistical Atlases and Computational Models of the Heart. ACDC and MMWHS Challenges - 8th International Workshop, STACOM 2017, Held in Conjunction with MICCAI 2017, Quebec City, Canada, September 10-14, 2017, Revised Selected Papers* (Springer), 130–139
- Payer, C., Štern, D., Bischof, H., and Urschler, M. (2018). Multi-label whole heart segmentation using CNNs and anatomical label configurations. In *International Workshop on Statistical Atlases and Computational Models of the Heart* (Springer International Publishing), 190–198
- Peng, B. and Zhang, L. (2012). Evaluation of image segmentation quality by adaptive ground truth composition. In *European Conference on Computer Vision* (Springer Berlin Heidelberg), 287–300. doi:10.1007/978-3-642-33712-3_21
- Peng, P., Lekadir, K., Gooya, A., Shao, L., Petersen, S. E., and Frangi, A. F. (2016). A review of heart chamber segmentation for structural and functional analysis using cardiac magnetic resonance imaging. *Magnetic Resonance Materials in Physics, Biology and Medicine* 29, 155—195. doi:10.1007/s10334-015-0521-4
- Petitjean, C., Zuluaga, M. A., Bai, W., Dacher, J.-N., Grosgeorge, D., Caudron, J., et al. (2015). Right ventricle segmentation from cardiac MRI: a collation study. *Medical image analysis* 19, 187–202. doi:10.1016/j.media.2014.10.004
- Poudel, R. P. K., Lamata, P., and Montana, G. (2016). Recurrent fully convolutional neural networks for multi-slice MRI cardiac segmentation. In *1st International Workshops on Reconstruction and Analysis of Moving Body Organs, RAMBO 2016 and 1st International Workshops on Whole-Heart and Great Vessel Segmentation from 3D Cardiovascular MRI in Congenital Heart Disease, HVSMR 2016*. 83–94
- Preetha, C. J., Haridasan, S., Abdi, V., and Engelhardt, S. (2018). Segmentation of the left atrium from 3D Gadolinium-Enhanced MR images with convolutional neural networks. In *Statistical Atlases and Computational Models of the Heart. Atrial Segmentation and LV Quantification Challenges* (Springer International Publishing), 265–272. doi:10.1007/978-3-030-12029-0_29
- Qin, C., Bai, W., Schlemper, J., Petersen, S. E., Piechnik, S. K., Neubauer, S., et al. (2018a). Joint learning of motion estimation and segmentation for cardiac mr image sequences. In *Medical Image Computing and Computer Assisted Intervention*. 472–480
- Qin, C., Bai, W., Schlemper, J., Petersen, S. E., Piechnik, S. K., Neubauer, S., et al. (2018b). Joint motion estimation and segmentation from undersampled cardiac MR image. In *Machine Learning for Medical Image Reconstruction* (Springer International Publishing), 55–63. doi:10.1007/978-3-030-00129-2_7
- Radau, P. and Others (2009). Evaluation framework for algorithms segmenting short axis cardiac MRI. *The MIDAS Journal - Cardiac MR Left Ventricle Segmentation Challenge* <http://www.cardiacatlas.org/studies/sunnybrook-cardiac-data/>
- Robinson, R., Valindria, V. V., Bai, W., Oktay, O., Kainz, B., Suzuki, H., et al. (2019). Automated quality control in image segmentation: application to the UK biobank cardiovascular magnetic resonance imaging study. *Journal of Cardiovascular Magnetic Resonance* 21, 18. doi:10.1186/s12968-019-0523-x
- Rohé, M.-M., Sermesant, M., and Pennec, X. (2017). Automatic Multi-Atlas segmentation of myocardium with SVF-Net. In *Statistical Atlases and Computational Models of the Heart. ACDC and MMWHS Challenges* (Springer International Publishing), 170–177. doi:10.1007/978-3-319-75541-0_18
- Ronneberger, F. P., Olaf and Brox, T. (2015). U-Net: Convolutional networks for biomedical image segmentation. In *Medical Image Computing and Computer Assisted Intervention* (Springer), 234–241
- Rueckert, D., Sonoda, L. I., Hayes, C., Hill, D. L., Leach, M. O., and Hawkes, D. J. (1999). Nonrigid registration using free-form deformations: application to breast MR images. *IEEE Transactions on Medical Imaging* 18, 712–721. doi:10.1109/42.796284

- Ruijsink, B., Puyol-Antón, E., Oksuz, I., Sinclair, M., Bai, W., Schnabel, J. A., et al. (2019). Fully automated, Quality-Controlled cardiac analysis from CMR: Validation and Large-Scale application to characterize cardiac function. *Journal of the American College of Cardiology* doi:10.1016/j.jcmg.2019.05.030
- Ryffel, T., Trask, A., Dahl, M., Wagner, B., Mancuso, J., Rueckert, D., et al. (2018). A generic framework for privacy preserving deep learning. In *Privacy preserving machine learning*. 1–8
- Sander, J., de Vos, B. D., Wolterink, J. M., and Išgum, I. (2019). Towards increased trustworthiness of deep learning segmentation methods on cardiac MRI. In *Medical Imaging 2019: Image Processing* (International Society for Optics and Photonics), vol. 10949, 1094919. doi:10.1117/12.2511699
- Santini, G., Della Latta, D., Martini, N., Valvano, G., Gori, A., Ripoli, A., et al. (2017). An automatic deep learning approach for coronary artery calcium segmentation. In *International Federation for Medical and Biological Engineering*. vol. 65, 374–377
- Savioli, N., Montana, G., and Lamata, P. (2018). V-FCNN: Volumetric fully convolution neural network for automatic atrial segmentation. In *Statistical Atlases and Computational Models of the Heart. Atrial Segmentation and LV Quantification Challenges* (Springer International Publishing), 273–281. doi:10.1007/978-3-030-12029-0_30
- Savioli, N., Vieira, M. S., Lamata, P., and Montana, G. (2018). Automated segmentation on the entire cardiac cycle using a deep learning work - flow. In *2018 Fifth International Conference on Social Networks Analysis, Management and Security (SNAMS)*. 153–158. doi:10.1109/SNAMS.2018.8554962
- Savioli, N., Vieira, M. S., Lamata, P., and Montana, G. (2018). A generative adversarial model for right ventricle segmentation. *Arxiv Preprint* abs/1810.03969. Available at <http://arxiv.org/abs/1810.03969> (Accessed September 1, 2019)
- Schaap, M., Metz, C. T., van Walsum, T., van der Giessen, A. G., Weustink, A. C., Mollet, N. R., et al. (2009). Standardized evaluation methodology and reference database for evaluating coronary artery centerline extraction algorithms. *Medical image analysis* 13, 701–714. doi:10.1016/j.media.2009.06.003. :<http://coronary.bigr.nl/centerlines/>
- Schlemper, J., Oktay, O., Bai, W., Castro, D. C., Duan, J., Qin, C., et al. (2018). Cardiac MR segmentation from undersampled k-space using deep latent representation learning. In *Medical Image Computing and Computer Assisted Intervention* (Springer International Publishing), 259–267. doi:10.1007/978-3-030-00928-1_30
- Shadmi, R., Mazo, V., Bregman-Amitai, O., and Elnekave, E. (2018). Fully-convolutional deep-learning based system for coronary calcium score prediction from non-contrast chest CT. In *International Symposium on Biomedical Imaging (IEEE)*, 24–28
- Shelhamer, E., Long, J., and Darrell, T. (2017). Fully convolutional networks for semantic segmentation. *IEEE transactions on pattern analysis and machine intelligence* 39, 640–651. doi:10.1109/TPAMI.2016.2572683
- Shen, D., Wu, G., and Suk, H.-I. (2017). Deep learning in medical image analysis. *Annual review of biomedical engineering* 19, 221–248
- Shen, Y., Fang, Z., Gao, Y., Xiong, N., Zhong, C., and Tang, X. (2019). Coronary arteries segmentation based on 3D FCN with attention gate and level set function. *IEEE Access* 7, 42826–42835
- Shi, Z., Zeng, G., Zhang, L., Zhuang, X., Li, L., Yang, G., et al. (2018). Bayesian VoxDRN: A probabilistic deep voxelwise dilated residual network for whole heart segmentation from 3D MR images. In *Medical Image Computing and Computer Assisted Intervention* (Springer International Publishing), 569–577. doi:10.1007/978-3-030-00937-3_65

- Simonyan, K. and Zisserman, A. (2015). Very deep convolutional networks for large-scale image recognition. In *International Conference on Learning Representations*. 14. doi:10.1016/j.infsof.2008.09.005
- Smistad, E. and Lindseth, F. (2014). Real-time tracking of the left ventricle in 3D ultrasound using kalman filter and mean value coordinates. *Medical Image Segmentation for Improved Surgical Navigation*, 189
- Smistad, E., Ostvik, A., Haugen, B. O., and Lovstakken, L. (2017). 2D left ventricle segmentation using deep learning. In *2017 IEEE International Ultrasonics Symposium (IUS)* (IEEE), 1–4
- Smistad, E., Østvik, A., Mjal Salte, I., Leclerc, S., Bernard, O., and Lovstakken, L. (2018). Fully automatic Real-Time ejection fraction and MAPSE measurements in 2D echocardiography using deep neural networks. In *2018 IEEE International Ultrasonics Symposium (IUS)* (IEEE), 1–4
- Srivastava, N., Hinton, G., Krizhevsky, A., Sutskever, I., and Salakhutdinov, R. (2014). Dropout: A simple way to prevent neural networks from overfitting. *Journal of machine learning research: JMLR* 15, 1929–1958
- Suinesiaputra, A., Cowan, B. R., Al-Agamy, A. O., Elattar, M. A., Ayache, N., Fahmy, A. S., et al. (2014). A collaborative resource to build consensus for automated left ventricular segmentation of cardiac MR images. *Medical image analysis* 18, 50–62. doi:10.1016/j.media.2013.09.001. <http://www.cardiacatlas.org/challenges/lv-segmentation-challenge/>
- Szegedy, C., Liu, W., Jia, Y., Sermanet, P., Reed, S., Anguelov, D., et al. (2015). Going deeper with convolutions. In *Conference on Computer Vision and Pattern Recognition*. 1–9
- Szegedy, C., Zaremba, W., Sutskever, I., Bruna, J., Erhan, D., Goodfellow, I., et al. (2014). Intriguing properties of neural networks. In *2nd International Conference on Learning Representations, ICLR 2014, Banff, AB, Canada, April 14-16, 2014, Conference Track Proceedings*. 1–10
- Tan, L. K., Liew, Y. M., Lim, E., and McLaughlin, R. A. (2017). Convolutional neural network regression for short-axis left ventricle segmentation in cardiac cine mr sequences. *Medical Image Analysis* 39, 78–86
- Tao, Q., Ipek, E. G., Shahzad, R., Berendsen, F. F., Nazarian, S., and van der Geest, R. J. (2016). Fully automatic segmentation of left atrium and pulmonary veins in late gadolinium-enhanced MRI: Towards objective atrial scar assessment. *Journal of magnetic resonance imaging* 44, 346–354. doi:10.1002/jmri.25148
- Tao, Q., Yan, W., Wang, Y., Paiman, E. H. M., Shamonin, D. P., Garg, P., et al. (2019). Deep learning-based method for fully automatic quantification of left ventricle function from cine MR images: A multivendor, multicenter study. *Radiology* 290, 180513. doi:10.1148/radiol.2018180513
- Tarroni, G., Oktay, O., Bai, W., Schuh, A., Suzuki, H., Passerat-Palmbach, J., et al. (2019). Learning-Based quality control for cardiac MR images. *IEEE Transactions on Medical Imaging* 38, 1127–1138. doi:10.1109/TMI.2018.2878509
- Tarroni, G., Oktay, O., Sinclair, M., Bai, W., Schuh, A., Suzuki, H., et al. (2018). A comprehensive approach for learning-based fully-automated inter-slice motion correction for short-axis cine cardiac MR image stacks. In *Medical Image Computing and Computer Assisted Intervention*. 268–276
- Tavakoli, V. and Amini, A. A. (2013). A survey of shaped-based registration and segmentation techniques for cardiac images. *Computer Vision and Image Understanding* 117, 966–989. doi:10.1016/j.cviu.2012.11.017
- Tobon-Gomez, C., Geers, A. J., Peters, J., Weese, J., Pinto, K., Karim, R., et al. (2015). Benchmark for algorithms segmenting the left atrium from 3D CT and MRI datasets. *IEEE transactions on medical imaging* 34, 1460–1473. doi:10.1109/TMI.2015.2398818. www.cardiacatlas.org/challenges/left-atrium-segmentation-challenge/

- Tong, Q., Ning, M., Si, W., Liao, X., and Qin, J. (2017). 3D deeply-supervised U-net based whole heart segmentation. In *International Workshop on Statistical Atlases and Computational Models of the Heart* (Springer), 224–232
- Tran, P. V. (2016). A fully convolutional neural network for cardiac segmentation in Short-Axis MRI. *Arxiv Preprint* abs/1604.00494. Available at <http://arxiv.org/abs/1604.00494> (Accessed September 1, 2019)
- Tziritas, G. and Grinias, E. (2017). Fast fully-automatic localization of left ventricle and myocardium in mri using mrf model optimization, substructures tracking and b-spline smoothing. In *International Workshop on Statistical Atlases and Computational Models of the Heart*. 91–100
- Van Der Geest, R. J. and Reiber, J. H. (1999). Quantification in cardiac MRI. *Journal of magnetic resonance imaging* 10, 602–608
- Vaswani, A., Shazeer, N., Parmar, N., Uszkoreit, J., Jones, L., Gomez, A. N., et al. (2017). Attention is all you need. In *Conference on Neural Information Processing Systems*, eds. I. Guyon, U. V. Luxburg, S. Bengio, H. Wallach, R. Fergus, S. Vishwanathan, and R. Garnett (Curran Associates, Inc.), 5998–6008
- Veni, G., Moradi, M., Bulu, H., Narayan, G., and Syeda-Mahmood, T. (2018). Echocardiography segmentation based on a shape-guided deformable model driven by a fully convolutional network prior. In *2018 IEEE 15th International Symposium on Biomedical Imaging (ISBI 2018)* (IEEE), 898–902
- Vesal, S., Ravikumar, N., and Maier, A. (2018). Dilated convolutions in neural networks for left atrial segmentation in 3D gadolinium Enhanced-MRI. In *Statistical Atlases and Computational Models of the Heart. Atrial Segmentation and LV Quantification Challenges - 9th International Workshop, STACOM 2018, Held in Conjunction with MICCAI 2018, Granada, Spain, September 16, 2018, Revised Selected Papers*. 319–328
- Vigneault, D. M., Xie, W., Ho, C. Y., Bluemke, D. A., and Noble, J. A. (2018). Ω -Net (Omega-Net): Fully automatic, multi-view cardiac MR detection, orientation, and segmentation with deep neural networks. *Medical Image Analysis* 48, 95–106. doi:10.1016/j.media.2018.05.008
- Volpi, R., Namkoong, H., Sener, O., Duchi, J. C., Murino, V., and Savarese, S. (2018). Generalizing to unseen domains via adversarial data augmentation. In *Conference on Neural Information Processing Systems*. 5339–5349
- Wang, C., MacGillivray, T., Macnaught, G., Yang, G., and Newby, D. (2018). A two-stage 3D unet framework for multi-class segmentation on full resolution image. *Arxiv Preprint* , 1–10 Available at <http://arxiv.org/abs/1804.04341> (Accessed September 1, 2019)
- Wang, C. and Smedby, Ö. (2017). Automatic whole heart segmentation using deep learning and shape context. In *Statistical Atlases and Computational Models of the Heart. ACDC and MMWHS Challenges - 8th International Workshop, STACOM 2017, Held in Conjunction with MICCAI 2017, Quebec City, Canada, September 10-14, 2017, Revised Selected Papers* (Springer), 242–249
- Wolterink, J. M., Leiner, T., de Vos, B. D., van Hamersvelt, R. W., Viergever, M. A., and Išgum, I. (2016). Automatic coronary artery calcium scoring in cardiac CT angiography using paired convolutional neural networks. *Medical Image Analysis* 34, 123–136
- Wolterink, J. M., Leiner, T., and Išgum, I. (2019a). Graph convolutional networks for coronary artery segmentation in cardiac CT angiography. *Arxiv Preprint* abs/1908.05343. Available at <http://arxiv.org/abs/1908.05343> (Accessed September 1, 2019)
- Wolterink, J. M., Leiner, T., Viergever, M. A., and Išgum, I. (2017a). Dilated convolutional neural networks for cardiovascular MR segmentation in congenital heart disease. In *Reconstruction, Segmentation, and Analysis of Medical Images*. 95–102

- Wolterink, J. M., Leiner, T., Viergever, M. A., and Išgum, I. (2017b). Generative adversarial networks for noise reduction in Low-Dose CT. *IEEE Transactions on Medical Imaging* 36, 2536–2545. doi:10.1109/TMI.2017.2708987
- Wolterink, J. M., Leiner, T., Viergever, M. A., and Išgum, I. (2017c). Automatic segmentation and disease classification using cardiac cine mr images. In *Statistical Atlases and Computational Models of the Heart. ACDC and MMWHS Challenges - 8th International Workshop, STACOM 2017, Held in Conjunction with MICCAI 2017, Quebec City, Canada, September 10-14, 2017, Revised Selected Papers*. vol. 10663 LNCS of *Lecture Notes in Computer Science (including subseries Lecture Notes in Artificial Intelligence and Lecture Notes in Bioinformatics)*, 101–110
- Wolterink, J. M., van Hamersvelt, R. W., Viergever, M. A., Leiner, T., and Išgum, I. (2019b). Coronary artery centerline extraction in cardiac CT angiography using a CNN-based orientation classifier. *Medical Image Analysis* 51, 46–60
- Xia, Q., Yao, Y., Hu, Z., and Hao, A. (2018). Automatic 3D atrial segmentation from GE-MRIs using volumetric fully convolutional networks. In *Statistical Atlases and Computational Models of the Heart. Atrial Segmentation and LV Quantification Challenges* (Springer International Publishing), 211–220. doi:10.1007/978-3-030-12029-0_23
- Xiong, Z., Fedorov, V. V., Fu, X., Cheng, E., Macleod, R., and Zhao, J. (2019). Fully automatic left atrium segmentation from late gadolinium enhanced magnetic resonance imaging using a dual fully convolutional neural network. *IEEE Transactions on Medical Imaging* 38, 515–524. doi:10.1109/TMI.2018.2866845
- Xu, C., Xu, L., Gao, Z., Zhao, S., Zhang, H., Zhang, Y., et al. (2018a). Direct delineation of myocardial infarction without contrast agents using a joint motion feature learning architecture. *Medical image analysis* 50, 82–94. doi:10.1016/j.media.2018.09.001
- Xu, Z., Wu, Z., and Feng, J. (2018b). CFUN: Combining faster R-CNN and U-net network for efficient whole heart segmentation. *Arxiv Preprint abs/1812.04914*. Available at <http://arxiv.org/abs/1812.04914> (Accessed September 1, 2019)
- Xue, W., Brahm, G., Pandey, S., Leung, S., and Li, S. (2018). Full left ventricle quantification via deep multitask relationships learning. *Medical Image Analysis* 43, 54–65. doi:10.1016/j.media.2017.09.005
- Yan, W., Wang, Y., Li, Z., van der Geest, R. J., and Tao, Q. (2018). Left ventricle segmentation via Optical-Flow- net from Short-Axis cine MRI : Preserving the temporal coherence of cardiac motion. In *Medical Image Computing and Computer Assisted Intervention* (Springer International Publishing), vol. 11073 LNCS, 613–621. doi:10.1007/978-3-030-00937-3_70
- Yang, G., Chen, J., Gao, Z., Zhang, H., Firmin, D., and others (2018a). Multiview sequential learning and dilated residual learning for a fully automatic delineation of the left atrium and pulmonary veins from late Gadolinium-Enhanced cardiac MRI images. In *Conf Proc IEEE Eng Med Biol Soc*. vol. 2018, 1123–1127. doi:10.1109/EMBC.2018.8512550
- Yang, G., Zhuang, X., Khan, H., Haldar, S., Nyktari, E., Li, L., et al. (2018b). Fully automatic segmentation and objective assessment of atrial scars for long-standing persistent atrial fibrillation patients using late gadolinium-enhanced MRI. *Medical physics* 45, 1562–1576. doi:10.1002/mp.12832
- Yang, G., Zhuang, X., Khan, H., Haldar, S., Nyktari, E., Ye, X., et al. (2017a). Segmenting atrial fibrosis from late Gadolinium-Enhanced cardiac MRI by Deep-Learned features with stacked sparse Auto-Encoders. In *Medical Image Understanding and Analysis* (Springer International Publishing), 195–206. doi:10.1007/978-3-319-60964-5_17

- Yang, H., Sun, J., Li, H., Wang, L., and Xu, Z. (2016). Deep fusion net for multi-atlas segmentation: Application to cardiac MR images. In *Medical Image Computing and Computer Assisted Intervention* (Springer International Publishing), 521–528. doi:10.1007/978-3-319-46723-8_60
- Yang, X., Bian, C., Yu, L., Ni, D., and Heng, P.-A. (2017b). 3D convolutional networks for fully automatic fine-grained whole heart partition. In *International Workshop on Statistical Atlases and Computational Models of the Heart* (Springer), 181–189
- Yang, X., Bian, C., Yu, L., Ni, D., and Heng, P.-A. (2017c). Class-Balanced deep neural network for automatic ventricular structure segmentation. In *Statistical Atlases and Computational Models of the Heart. ACDC and MMWHS Challenges* (Springer International Publishing), 152–160. doi:10.1007/978-3-319-75541-0_16
- Yang, X., Bian, C., Yu, L., Ni, D., and Heng, P.-A. (2017d). Hybrid loss guided convolutional networks for whole heart parsing. In *International Workshop on Statistical Atlases and Computational Models of the Heart* (Springer), 215–223
- Ye, C., Wang, W., Zhang, S., and Wang, K. (2019). Multi-depth fusion network for whole-heart CT image segmentation. *IEEE Access* 7, 23421–23429
- Yu, F. and Koltun, V. (2016). Multi-Scale context aggregation by dilated convolutions. In *International Conference on Learning Representations*. 1–13
- Yu, L., Cheng, J.-Z., Dou, Q., Yang, X., Chen, H., Qin, J., et al. (2017a). Automatic 3D cardiovascular MR segmentation with Densely-Connected volumetric ConvNets. In *Medical Image Computing and Computer Assisted Intervention* (Springer International Publishing), 287–295. doi:10.1007/978-3-319-66185-8_33
- Yu, L., Guo, Y., Wang, Y., Yu, J., and Chen, P. (2017b). Segmentation of fetal left ventricle in echocardiographic sequences based on dynamic convolutional neural networks. *IEEE Trans. Biomed. Eng.* 64, 1886–1895
- Yu, L., Wang, S., Li, X., Fu, C.-W., and Heng, P.-A. (2019). Uncertainty-aware self-ensembling model for semi-supervised 3D left atrium segmentation. In *Medical Image Computing and Computer Assisted Intervention*. 605–613
- Yue, Q., Luo, X., Ye, Q., Xu, L., and Zhuang, X. (2019). Cardiac segmentation from LGE MRI using deep neural network incorporating shape and spatial priors. In *Medical Image Computing and Computer Assisted Intervention*. 559–567
- Zabihollahy, F., White, J. A., and Ukwatta, E. (2018). Myocardial scar segmentation from magnetic resonance images using convolutional neural network. In *Medical Imaging 2018: Computer-Aided Diagnosis* (International Society for Optics and Photonics), vol. 10575, 105752Z. doi:10.1117/12.2293518
- Zhang, D. P. (2010). *Coronary artery segmentation and motion modelling*. Ph.D. thesis, Imperial College London
- Zhang, J., Du, J., Liu, H., Hou, X., Zhao, Y., and Ding, M. (2019a). LU-NET: An improved U-Net for ventricular segmentation. *IEEE Access* 7, 92539–92546. doi:10.1109/ACCESS.2019.2925060
- Zhang, J., Gajjala, S., Agrawal, P., Tison, G. H., Hallock, L. A., Beussink-Nelson, L., et al. (2018a). Fully automated echocardiogram interpretation in clinical practice: feasibility and diagnostic accuracy. *Circulation* 138, 1623–1635
- Zhang, L., Karanikolas, G. V., Akçakaya, M., and Giannakis, G. B. (2018b). Fully automatic segmentation of the right ventricle via Multi-Task deep neural networks. In *IEEE International Conference on Acoustics, Speech and Signal Processing*. 6677–6681. doi:10.1109/ICASSP.2018.8461556

- Zhang, L., Wang, X., Yang, D., Sanford, T., Harmon, S., Turkbey, B., et al. (2019b). When unseen domain generalization is unnecessary? rethinking data augmentation. *Arxiv Preprint* abs/1906.03347. Available at <http://arxiv.org/abs/1906.03347> (Accessed September 1, 2019)
- Zhang, W., Zhang, J., Du, X., Zhang, Y., and Li, S. (2019c). An end-to-end joint learning framework of artery-specific coronary calcium scoring in non-contrast cardiac CT. *Computing* 101, 667–678
- Zhao, A., Balakrishnan, G., Durand, F., Guttag, J. V., and Dalca, A. V. (2019). Data augmentation using learned transformations for one-shot medical image segmentation. In *Conference on Computer Vision and Pattern Recognition*. 8543–8553
- [Dataset] Zhao, X. Z., J. (2018). 2018 left atrial segmentation challenge dataset. <http://atriaseg2018.cardiacatlas.org/>
- Zheng, Q., Delingette, H., and Ayache, N. (2019). Explainable cardiac pathology classification on cine MRI with motion characterization by semi-supervised learning of apparent flow. *Medical Image Analysis* 56, 80–95. doi:10.1016/j.media.2019.06.001
- Zheng, Q., Delingette, H., Duchateau, N., and Ayache, N. (2018). 3-D consistent and robust segmentation of cardiac images by deep learning with spatial propagation. *IEEE Transactions on Medical Imaging* 37, 2137–2148. doi:10.1109/TMI.2018.2820742
- Zheng, Y., Barbu, A., Georgescu, B., Scheuering, M., and Comaniciu, D. (2008). Four-chamber heart modeling and automatic segmentation for 3-D cardiac CT volumes using marginal space learning and steerable features. *IEEE Transactions on Medical Imaging* 27, 1668–1681
- Zhou, L., Deng, W., and Wu, X. (2019). Robust image segmentation quality assessment without ground truth. *Arxiv Preprint* abs/1903.08773. Available at <http://arxiv.org/abs/1903.08773> (Accessed September 1, 2019)
- Zhou, X.-Y. and Yang, G.-Z. (2019). Normalization in training U-Net for 2D biomedical semantic segmentation. *IEEE Robotics and Automation Letters* PP, 1–1. doi:10.1109/LRA.2019.2896518
- Zhuang, X., Li, L., Payer, C., Stern, D., Urschler, M., Heinrich, M. P., et al. (2019). Evaluation of algorithms for Multi-Modality whole heart segmentation: An Open-Access grand challenge. *Medical Image Analysis* 58, 101537. doi:<https://doi.org/10.1016/j.media.2019.101537>. <http://www.sdspeople.fudan.edu.cn/zhuangxiahai/0/mmwhs17/>
- Zhuang, X., Rhode, K. S., Razavi, R. S., Hawkes, D. J., and Ourselin, S. (2010). A registration-based propagation framework for automatic whole heart segmentation of cardiac MRI. *IEEE Transactions on Medical Imaging* 29, 1612–1625. doi:10.1109/TMI.2010.2047112
- Zotti, C., Luo, Z., Lalande, A., Humbert, O., and Jodoin, P.-M. (2017). GridNet with automatic shape prior registration for automatic MRI cardiac segmentation. In *International Workshop on Statistical Atlases and Computational Models of the Heart*. 73–81
- Zotti, C., Luo, Z., Lalande, A., and Jodoin, P.-M. (2019). Convolutional neural network with shape prior applied to cardiac MRI segmentation. *IEEE Journal of Biomedical and Health Informatics* 23, 1119–1128. doi:10.1109/JBHI.2018.2865450
- Zreik, M., Leiner, T., De Vos, B. D., Van Hamersvelt, R. W., Viergever, M. A., and Išgum, I. (2016). Automatic segmentation of the left ventricle in cardiac CT angiography using convolutional neural networks. In *International Symposium on Biomedical Imaging*. 40–43
- Zreik, M., Lessmann, N., van Hamersvelt, R. W., Wolterink, J. M., Voskuil, M., Viergever, M. A., et al. (2018a). Deep learning analysis of the myocardium in coronary CT angiography for identification of patients with functionally significant coronary artery stenosis. *Medical Image Analysis* 44, 72–85
- Zreik, M., van Hamersvelt, R. W., Wolterink, J. M., Leiner, T., Viergever, M. A., and Išgum, I. (2018b). A recurrent CNN for automatic detection and classification of coronary artery plaque and stenosis in

coronary CT angiography. *IEEE Transactions on Medical Imaging* 38, 1588–1598. doi:10.1109/TMI.2018.2883807